

Biological and climate controls on North Atlantic marine carbon dynamics over the last millennium: Insights from an absolutely-dated shell based record from the North Icelandic Shelf

Richardson, Christopher; Reynolds, David; Scourse, James; Butler, Paul; Wanamaker, Alan; Hall, Ian R.

Global Biogeochemical Cycles

DOI:

[10.1002/2017GB005708](https://doi.org/10.1002/2017GB005708)

Published: 01/12/2017

Peer reviewed version

[Cyswllt i'r cyhoeddiad / Link to publication](#)

Dyfyniad o'r fersiwn a gyhoeddwyd / Citation for published version (APA):

Richardson, C., Reynolds, D., Scourse, J., Butler, P., Wanamaker, A., & Hall, I. R. (2017). Biological and climate controls on North Atlantic marine carbon dynamics over the last millennium: Insights from an absolutely-dated shell based record from the North Icelandic Shelf. *Global Biogeochemical Cycles*, 31(12), 1718-1735. <https://doi.org/10.1002/2017GB005708>

Hawliau Cyffredinol / General rights

Copyright and moral rights for the publications made accessible in the public portal are retained by the authors and/or other copyright owners and it is a condition of accessing publications that users recognise and abide by the legal requirements associated with these rights.

- Users may download and print one copy of any publication from the public portal for the purpose of private study or research.
- You may not further distribute the material or use it for any profit-making activity or commercial gain
- You may freely distribute the URL identifying the publication in the public portal ?

Take down policy

If you believe that this document breaches copyright please contact us providing details, and we will remove access to the work immediately and investigate your claim.

Title: Biological and climate controls on North Atlantic marine carbon dynamics over the last millennium: Insights from an absolutely-dated shell based record from the North Icelandic Shelf

Authors: Reynolds D.J.¹, Hall, I.R.¹, Scourse, J.D.², Richardson, C.A.³, Wanamaker, A.D.⁴, and Butler, P.G.^{2/3}

Affiliations:

¹School of Earth and Ocean Sciences, Cardiff University, Cardiff, CF10 3AT, UK.

²College of Life and Environmental Sciences, University of Exeter, Penryn Campus, Penryn, TR10 9EZ, UK.

³School of Ocean Sciences, College of Natural Science, Bangor University, Menai Bridge, Anglesey, LL59 5AB, UK.

⁴Department of Geological and Atmospheric Sciences, Iowa State University, Ames, Iowa, 50011-3212, USA.

*Correspondence to: reynoldsd3@cardiff.ac.uk

Ian Hall Hall@cardiff.ac.uk

James Scourse j.scourse@exeter.ac.uk

Alan D. Wanamaker Jr. adw@iastate.edu

Christopher Richardson c.a.richardson@bangor.ac.uk

Paul Butler p.g.butler@bangor.ac.uk

Keywords: Carbon isotopes, North Atlantic, *Arctica islandica*, sclerochronology, productivity, NAO

Abstract

Given the rapid increase in atmospheric carbon dioxide concentrations ($p\text{CO}_2$) over the industrial era there is a pressing need to construct long term records of natural carbon cycling prior to this perturbation and to develop a more robust understanding of the role the oceans play in the sequestration of atmospheric carbon. Here we reconstruct the historical biological and climatic controls on the carbon isotopic ($\delta^{13}\text{C}$ -shell) composition of the North Icelandic shelf waters over the last millennium derived from the shells of the long-lived marine bivalve mollusc *Arctica islandica*. Variability in the annually resolved $\delta^{13}\text{C}$ -shell record is dominated by multi-decadal variability with a negative trend ($-0.003 \pm 0.002\text{‰yr}^{-1}$) over the industrial era (1800-2000 CE). This trend is consistent with the marine Suess effect brought about by the sequestration of isotopically light carbon ($\delta^{13}\text{C}$ of CO_2) derived from the burning of fossil fuels. Comparison of the $\delta^{13}\text{C}$ -shell record with contemporary proxy archives, over the last millennium, and instrumental data over the 20th century, highlight that both biological (primary production) and physical environmental factors such as relative shifts in the proportion of Subpolar Mode Waters and Arctic Intermediate Waters entrained onto the North Icelandic shelf, atmospheric circulation patterns associated with the winter North Atlantic Oscillation, and subpolar gyre sea surface temperatures and salinity, are the likely mechanisms that contribute to natural variations in seawater $\delta^{13}\text{C}$ variability on the North Icelandic shelf. Contrasting $\delta^{13}\text{C}$ fractionation processes associated with these biological and physical mechanisms likely cause the attenuated local marine Suess effect signal at this locality.

1. Introduction

Over the last 150 years, especially the last 50 years, atmospheric $p\text{CO}_2$ levels have increased exponentially due to anthropogenic activities, namely burning fossil fuels (IPCC, 2013). In contrast to variations in CO_2 emissions, atmospheric $p\text{CO}_2$ show considerable variation on an inter-annual timescale indicating that CO_2 exchange between the different components of the climate system is temporally variable and likely influenced by climate variability and the strength of the biological pump (Conway et al., 1994, Peylin et al., 2005, McKinley et al., 2004). The global oceans play an important role in this inter-annual CO_2 variability due to the large carbon storage capacity of the oceans, the large gross rate of air-sea CO_2 exchange relative to the net flux of air-sea CO_2 exchange (80 PgC yr^{-1} relative to $2.3 \pm 0.7 \text{ PgC yr}^{-1}$, $1 \text{ PgC} = 10^{15} \text{ gC}$; IPCC, 2013) and the rapid rate (one year) in which the surface oceans reach $p\text{CO}_2$ equilibrium (Broecker and Peng, 1974), although they take considerably longer to reach isotopic equilibrium (10-11 years) (Galbraith et al., 2015, Broecker and Peng, 1974). Recent studies have estimated that the global oceans have sequestered approximately half of the anthropogenically produced CO_2 (Sabine et al., 2004). However, there is considerable spatial variability, with the North Atlantic in particular taking up $\sim 23\%$ of the total air-sea CO_2 flux, despite representing just 15% of the global ocean surface area (Sabine et al., 2004). It is thought that regions of deep water convection, such as the Labrador Sea, are likely responsible for the relatively high uptake of CO_2 across the subpolar region (DeGrandpre et al., 2006). The influence of sequestered anthropogenic CO_2 , as well as reducing ocean pH levels (Doney et al., 2009), is reflected in the change of the carbon isotopic ($^{12}\text{C}/^{13}\text{C}$; $\delta^{13}\text{C}$) composition of seawater dissolved inorganic carbon ($\delta^{13}\text{C}_{\text{DIC}}$) which has become isotopically lighter (lower) over the 19th and 20th centuries. This isotopic trend is from anthropogenic CO_2 produced from largely plant-derived fossil fuels, which have nominal $\delta^{13}\text{C}$ values around -27‰ (Peterson and Fry, 1987) and is known as the marine Suess effect (after Suess, 1953, also see Keeling et al., 2005). The Suess effect has been detected in numerous marine proxy archives (e.g.

Nozaki et al., 1978, Bohm et al., 1996, Bohm et al., 2002, Butler et al., 2009, Cage and Austin, 2010, Swart et al., 2010, Schöne et al., 2011), which provides a unique opportunity to evaluate rates of carbon incorporation into biocarbonates across ocean basins.

Despite the importance of the global oceans in the sequestration of atmospheric $p\text{CO}_2$, large uncertainties remain, particularly in the temperate to subpolar latitudes, as to what drives inter-annual variability in air-sea CO_2 exchange (Ullman et al., 2009). In part our understanding is constrained by the relative brevity of the observational record (typically back to 1970; Gruber et al., 1999) and the lack of absolutely-dated marine based proxy archives (Beirne et al., 2012). There is therefore a need to develop robust records of carbon dynamics, including spatial and temporal variability, in the temperate and subpolar oceans prior to the instrumental period.

In recent years sclerochronological records derived from long-lived marine bivalve molluscs have demonstrated potential to provide novel insights into the role the oceans play in the global climate system over past centuries to millennia. The development of millennial length absolutely-dated annually-resolved growth increment width sclerochronologies (Butler et al., 2013) and stable isotope series (Reynolds et al., 2016) provide the opportunity to investigate marine variability from the subpolar North Atlantic region over intervals that extend well beyond the industrial period (pre-1800 CE). Such records therefore allow the examination of naturally forced marine climate variability during periods prior to the establishment of a pronounced anthropogenic influence. The utility of long-lived marine bivalves, in particular *Arctica islandica*, as archives of past climatic variability is based on five key attributes: 1) They can attain maximum longevities in excess of 500 years (Butler et al., 2013) meaning only a limited number of shells is required to extend the records back beyond the instrumental observational period; 2) The shells form growth increments on a proven annual basis (Witbaard et al., 1994), equivalent in many ways to tree rings; 3) Shell growth is synchronous amongst co-extant individuals and populations facilitating the application of cross-dating statistical techniques, derived from dendrochronology, for dating fossil specimens relative to live-collected individuals whose date of death is known (Marchitto et al., 2000, Scourse et al., 2006, Butler et al., 2013, Mette et al., 2016). These techniques facilitate the construction of absolutely dated chronologies that can extend beyond the life span of one individual allowing the extension of the records over hundreds of years (Butler et al., 2013). 4) Changes in ambient seawater geochemistry ($\delta^{18}\text{O}$ and $\delta^{13}\text{C}$) are recorded in the shell matrix during calcium carbonate precipitation (Schöne et al., 2005, Wanamaker et al., 2008b, Schöne et al., 2011, Wanamaker et al., 2011, Beirne et al., 2012, Reynolds et al., 2016). 5) The size and number of shells included in chronologies provides the possibility of generating replicate analyses that facilitate a more robust characterisation and quantification of reconstruction uncertainties.

The $\delta^{13}\text{C}$ composition of *A. islandica* shells ($\delta^{13}\text{C}$ -shell) has been empirically shown to reflect changes in the $\delta^{13}\text{C}$ composition of $\delta^{13}\text{C}_{\text{DIC}}$ (Equ. 1) in the ambient seawater bathing the shell, coupled with a small component of respiratory and metabolic $\delta^{13}\text{C}$ ($\delta^{13}\text{C}_{\text{R}}$ and $\delta^{13}\text{C}_{\text{M}}$ respectively; Beirne et al., 2012).

$$\text{Equ. 1.} \quad \delta^{13}\text{C}_{\text{DIC}} = \delta^{13}\text{C-shell} - 1.0 (\pm 0.30\text{‰}) \quad (\text{Beirne et al., 2012})$$

Whilst it is generally accepted that the $\delta^{13}\text{C}_{\text{R}}$ and $\delta^{13}\text{C}_{\text{M}}$ (collectively termed vital effects) component of $\delta^{13}\text{C}$ -shell variability are negligible over the majority of the shell records, there is debate as to whether during the early years of shell growth (~ first 20 to 40 years for *A. islandica*) these vital effects may mask variability in the ambient seawater chemistry (Butler et al., 2011, Schöne et al., 2011). Despite the work of Beirne et al. (2012), these uncertainties still persist due to the relatively small number of shells that have been used to examine the influence of these vital effects on $\delta^{13}\text{C}$ -shell variability across space and time.

In the marine environment variability in $\delta^{13}\text{C}_{\text{DIC}}$ is controlled by fractionation processes occurring during air-sea CO_2 exchange and primary production (Lynch-stieglitz et al., 1995). During time intervals, or in geographical areas, characterised by the increased (decreased) oceanic uptake of CO_2 , through air-sea exchange, this results in a negative (positive) shift in $\delta^{13}\text{C}_{\text{DIC}}$ values (Lynch-Stieglitz et al., 1995). Variability in primary production influences $\delta^{13}\text{C}_{\text{DIC}}$ through the process of photosynthesis in the near surface photic zone of the marine environment. During periods of high (low) primary production phytoplankton preferentially utilize $^{12}\text{C}_{\text{DIC}}$ versus $^{13}\text{C}_{\text{DIC}}$, resulting in a positive (negative) shift in seawater $\delta^{13}\text{C}_{\text{DIC}}$. In the context of these processes, the development of long-term baseline records of $\delta^{13}\text{C}_{\text{DIC}}$ variability, in conjunction with other independent archives of primary production and marine and atmospheric climate variability, could lead to a better understanding of the role climate variability plays in driving air-sea CO_2 exchange. $\delta^{13}\text{C}_{\text{DIC}}$ of seawater at any one location can also be impacted by physical processes not related to primary production including upwelling, riverine input, advection of water masses, and air-sea exchange rates (e.g., Zeebe and Wolf-Gladrow, 2001).

Here we examine $\delta^{13}\text{C}$ -shell variability in *A. islandica* shells collected on the North Icelandic shelf (Figure 1). This region is hydrographically important given the juxtaposition between two distinct North Atlantic water masses, Subpolar Mode Water (SPMW) and Arctic Intermediate Water (AIW) that influence the sample location. Variability in the proportion of SPMW and AIW water entrained onto the North Icelandic shelf through the interplay between the Irminger Current (IC) and the East Greenland Current/East Iceland Current (EGC/EIC) has a profound influence on both regional climate and primary production (Gudmundsson, 1998, Eiriksson et al., 2011, Vage et al., 2011, Wanamaker et al., 2012, Logemann et al., 2013, Reynolds et al., 2016). Given the availability of annually-resolved absolutely-dated proxy archives from this region (Butler et al., 2013, Reynolds et al., 2016) and the, albeit lower resolution, index of water mass composition (based on marine radiocarbon reservoir ages $[\Delta R]$; Wanamaker et al., 2012) this region is an ideal locality for assessing the potential climatic influences on $\delta^{13}\text{C}_{\text{DIC}}$ variability. Specifically, we aim to i) assess the uncertainties within the $\delta^{13}\text{C}$ -shell associated with changing vital effects over the early period of *A. islandica* shell growth; ii) to produce a 1000-year annually resolved $\delta^{13}\text{C}$ -shell record that faithfully records $\delta^{13}\text{C}_{\text{DIC}}$ and iii) to assess the environmental controls on the $\delta^{13}\text{C}_{\text{DIC}}$ variability on the North Icelandic shelf over both the modern instrumental period and the last 1000 years.

2. Methods

2.1 Sample collection, carbon isotope analysis and uncertainty

We examined the $\delta^{13}\text{C}$ composition of annually resolved aragonite shell samples micromilled from the annual growth increments of *A. islandica* shells collected, by means of mechanical dredge, from the North Icelandic shelf ($66^\circ 31.59' \text{ N}$, $18^\circ 11.74' \text{ W}$; shells collected from 80 m water depth; Figure 1; see Wanamaker et al., 2008a). The calendar age of each sample was derived using the North Iceland *A. islandica* growth increment width chronology that had been previously constructed using dendrochronological crossdating techniques and validated using radiocarbon dating (see Butler et al., 2013). The crossdating process assigns absolute calendar ages to each individual year providing a temporal framework for the isotopic analyses. Individual aragonite samples were micromilled using an ESI New Wave micromill and tungsten carbide drill bits from a total of 21 individual shells. The samples analysed covered the period from 953 to 2000 CE. Each sample was analysed using a Kiel IV carbonate preparation device coupled online to a Thermo Finnegan MAT 253 mass spectrometer. All stable isotopic measurements are reported in standard notation, relative to Vienna Pee Dee belemnite (V-PDB). Analytical precision was estimated to be $\pm 0.05\text{‰}$ ($\pm 1\sigma$) for $\delta^{13}\text{C}$ by measuring eight standards

(NBS-19) with each set of 38 samples. In addition to the analytical uncertainty in the $\delta^{13}\text{C}$ -shell measurement, other sources of uncertainty arise because of the potential influence of ontogenetic related vital effects and inter- and intra-shell variability (which incorporates sampling precision and natural $\delta^{13}\text{C}$ variability within and between shells). These additional sources of uncertainty were quantified using replicate samples drilled from the same calendar year in multiple shells, independent samples drilled from the same year in the same shell and the reanalysis of the single samples.

In order to assess the uncertainty in the annually-resolved $\delta^{13}\text{C}$ -shell record created by ontogenetic vital effects (age or growth related biological effects associated to changes in metabolic and respiratory carbon fractionation processes), the $\delta^{13}\text{C}$ -shell data of each individual shell were normalised to a mean of zero, to remove any long-term shift in $\delta^{13}\text{C}$, and the data aligned by growth increment number starting from the first increment in each shell corresponding to the first year of shell growth (ontogenetically aligned, Figure 2A). The arithmetic mean, standard deviation (σ) and standard error (SE) were then calculated using the ontogenetically aligned $\delta^{13}\text{C}$ -shell data to generate a standardised population mean ontogenetic $\delta^{13}\text{C}$ curve (Figure 2B) that could be compared to mean population shell growth rates. Averaging the $\delta^{13}\text{C}$ -shell data in this way facilitates the generation of a standardised population mean $\delta^{13}\text{C}$ curve. As the $\delta^{13}\text{C}$ -shell data were aligned by ontogenetic age (increment number) and not absolute calendar date it is possible to examine trends in $\delta^{13}\text{C}$ -shell associated with age and shell growth rates. This is possible as age related trends in $\delta^{13}\text{C}$ present in each of the shells, associated with common age or growth fractionation processes, are preserved during the averaging process and generation of the mean $\delta^{13}\text{C}$ curve whilst climate related $\delta^{13}\text{C}$ trends, which are randomised within the ontogenetically (rather than absolute calendar date) aligned data, are removed. Nonetheless examination of shells from the same time interval and of a similar age can result in ontogenetic and climate trends being aligned, leading to the false identification of ontogenetic variability. For instance, if only shells that lived over the industrial period were used in these analyses the averaging process may still preserve the negative $\delta^{13}\text{C}$ trend associated with the marine Suess effect giving the false impression that a negative ontogenetic trend in $\delta^{13}\text{C}$ exists. In order to avoid this potential artefact, we used $\delta^{13}\text{C}$ -shell data spanning a broad temporal range (953-2000 CE). This sampling strategy largely mitigates against any potential bias caused by the incorporation of residual climate trends that may have “survived” a more temporally constrained shell averaging process. Our method ensures that, providing a sufficient number of shells were analysed, any significant trends contained in the standardised population mean $\delta^{13}\text{C}$ curve are solely a result of ontogenetic vital effects. We evaluated the number of shells required for the analysis by examining the influence of sample depth (number of shells for any given increment number analysed) on the SE of the standardised population mean ontogenetic $\delta^{13}\text{C}$ curve generated using different numbers of shells. The standardised population mean ontogenetic $\delta^{13}\text{C}$ curve is only robust during periods with sufficient sample depth to result in a relatively low and stable SE (Figure 2D).

Trends in the standardised population mean ontogenetic $\delta^{13}\text{C}$ curve were assessed using linear regression analysis. The standardised population mean ontogenetic $\delta^{13}\text{C}$ curve was low pass filtered using a 10-year first order loess low pass filter in order to reduce the high frequency noise associated with the ontogenetic signal and the first order differential calculated. A change in sign of the first order differential therefore indicates a switch in the trend of the standardised population mean ontogenetic $\delta^{13}\text{C}$ curve. Linear regression analyses were used to evaluate trends in the standardised population mean ontogenetic $\delta^{13}\text{C}$ curve with respect to ontogenetic age.

2.3 Constructing the 1000 year $\delta^{13}\text{C}$ record and trend analyses

Given that the length of the record exceeds the maximum longevity of any single individual shell, in order to construct the complete millennial record the isotopic composition of multiple shells had to be examined and spliced together to create a single series. We adopted the same methodology in constructing the $\delta^{13}\text{C}$ -shell record that was employed in the generation of the 1047-year $\delta^{18}\text{O}$ -shell record (see Figure 7B, Reynolds et al., 2016). In total 1492 annually resolved aragonite samples were analysed spanning the 1047-year period. Replicate samples were analysed from the same years in multiple shells and from the reanalysis of single samples and material re-drilled from the same increment multiple times. The arithmetic mean of all replicate samples was calculated in each year containing replicate samples, including transition periods between shells, in order to generate a series containing one $\delta^{13}\text{C}$ -shell value per year for 1047 continuous years. Other than the averaging of replicate samples to create the single series, no additional statistical treatments were employed in the generation of the annually resolved 1047-year $\delta^{13}\text{C}$ -shell record.

We examined variability in the annually resolved 1047-year $\delta^{13}\text{C}$ -shell record using a suite of time series analysis techniques. To assess differences in the mean state of $\delta^{13}\text{C}$ -shell variability through time the series was binned into 50-year non-overlapping bins and the arithmetic mean and standard deviation calculated. To evaluate the spectral characteristics in the $\delta^{13}\text{C}$ -shell record we utilised a multi-taper method (MTM) spectral analysis and wavelet analysis. The MTM analysis was conducted in K-spectra v3.5 using three tapers and the 95% significance level calculated relative to red noise. The wavelet analysis was conducted in PAST v3 using the Morlet function.

2.4 Environmental analyses

2.4.1 Removing the marine Suess effect

Prior to evaluating the coherence between the $\delta^{13}\text{C}$ -shell record and environmental parameters it was first necessary to remove variability associated with the marine Suess effect, as this is associated with changing atmospheric $\delta^{13}\text{C}$ ratios rather than climate variability. The marine Suess effect signal, which is typically characterised by a negative trend and lowering in $\delta^{13}\text{C}$ values over the last ~ 150 years, was removed from the annually resolved $\delta^{13}\text{C}$ -shell record using two approaches. Firstly, for the comparison with modern observational datasets over the 20th century a linear detrending approach was applied to both the $\delta^{13}\text{C}$ -shell record and to the observational datasets. This approach allowed for the Suess effect trend to be removed without the loss of data typical of applying rectangular or Gaussian based filtering approaches. However, the linear detrending approach was not suitable for the removal of the Suess effect from the entire record, due to the generally exponential nature of the effect. Therefore, for the comparison of the $\delta^{13}\text{C}$ -shell record with contemporaneous proxy archives we applied a 100-year first order loess high pass filter. In the remainder of this paper the marine Suess effect detrended $\delta^{13}\text{C}$ -shell record will be referred to as $\delta^{13}\text{C}$ -shell_{detrend}.

2.4.2 Environmental analyses

To assess the ability of the $\delta^{13}\text{C}$ -shell to faithfully record the $\delta^{13}\text{C}_{\text{DIC}}$ of the seawater bathing the shell at the time of formation the $\delta^{13}\text{C}$ -shell_{detrend} record was compared with an index of onshore and oceanic phytoplankton productivity measured in the North Icelandic Sea (Gudmundsson, 1998). Whilst these data were available over the period 1958-1994 CE, a shift in the timing of the phytoplankton productivity surveys after 1985 has likely biased the record so that subsequently it does not accurately reflect true primary production variability (Gudmundsson, 1998). We therefore conducted linear regression analyses between the $\delta^{13}\text{C}$ -shell_{detrend} and the onshore and offshore phytoplankton

productivity records over the period 1958-1985 CE. Given the $\delta^{13}\text{C}$ -shell data was detrended to remove the Suess effect signal the phytoplankton productivity record was also linearly detrended.

The coherence between the $\delta^{13}\text{C}$ -shell_{detrend} record and oceanographic and atmospheric instrumental observational records was examined over the 20th century using correlation analyses. Correlation analyses were conducted between the $\delta^{13}\text{C}$ -shell_{detrend} record and linear detrended sea surface temperatures (SSTs) in the HadISST1 gridded dataset (Rayner et al., 2003), sea surface salinities (SSS) in the UKMO EN4 gridded SSS dataset (Good et al., 2013), sea level pressure (SLP) expressed as the winter North Atlantic Oscillation (wNAO; Trenberth and Paolino, 1980, Allan and Ansell, 2006), and sea ice extent in the HadISST1 gridded sea ice record (Rayner et al., 2003). The correlations, conducted using the KNMI Climate explorer facility (see Trouet and Van Oldenborgh, 2013), were calculated over the period 1900-2000 CE.

Linear regression and lead-lag correlation analyses were used to evaluate the strength and timing of the correlations identified using the results of the correlation analyses against the gridded environmental datasets. These analyses were conducted using the regional mean SST, SSS and sea ice extent data for regions highlighted as containing a significant correlation with the $\delta^{13}\text{C}$ -shell_{detrend} record. For the analysis of SLP we utilised an existing wNAO index derived from the HadSLP2 dataset (Allan and Ansell, 2006). Correlations were calculated over the period from 1900-2000 CE using linear detrended data. To evaluate the combined influence of the environmental variables on the $\delta^{13}\text{C}$ -shell record multiple linear regression model analyses were also conducted. The analyses, conducted using R-statistics version 3.4.1, incorporated subpolar gyre SSTs, SSS and the wNAO index. The analyses were conducted over the entire 20th century using linear detrended data.

The $\delta^{13}\text{C}$ -shell and $\delta^{13}\text{C}$ -shell_{detrend} data were compared with proxy archives for wNAO (Trouet et al., 2009, Ortega et al., 2015). To account for auto-correlation that can lead to amplified significance levels, the linear regression analyses were calculated using the Ebisuzaki Monte Carlo methodology (Ebisuzaki, 1997). Finally, both the $\delta^{13}\text{C}$ -shell and $\delta^{13}\text{C}$ -shell_{detrend} were compared with other co-registered sclerochronological archives from the North Icelandic shelf, including the negative exponential and regional curve standardisation detrended growth increment chronologies (referred to hereafter as the NE and RCS chronologies; Butler et al., 2013), the $\delta^{18}\text{O}$ -shell record (Reynolds et al., 2016) and the marine radiocarbon (^{14}C) reservoir age (ΔR) derived water mass proxy (Wanamaker et al., 2012). The ΔR series was derived by comparing the calibrated ^{14}C ages of shell material sampled from growth increments that had been precisely aged by means of sclerochronological crossdating (Wanamaker et al., 2012). Given the differences in the ^{14}C age of SPMW and AIW, relative shifts in the ^{14}C derived ages relative to the sclerochronologically derived ages facilitates the reconstruction of the relative composition of the water masses that are bathing the shells at the time of shell formation (Wanamaker et al., 2012). As the carbonate mass required for ^{14}C analyses is relatively large they incorporated a number of growth increments in each sample. Therefore, for comparison with the ΔR record the correlations were calculated using 50-year low pass filtered $\delta^{13}\text{C}$ -shell data from only the contemporaneous years containing ΔR data. A 50-year low pass filter was applied to the $\delta^{13}\text{C}$ -shell data to approximately match the resolution of the ΔR record.

To test the hypothesis that a proportion of the variability captured by the $\delta^{13}\text{C}$ -shell data is associated to the variability in SPMW advected through the Irminger Current, the $\delta^{13}\text{C}$ -shell data was correlated against subpolar gyre SSTs reconstructed from the analyses of planktonic foraminifera (*Globorotalia*

inflata) from the sediment core RAPiD-17-5P collected from south of Iceland (61° 28.900 N, 19° 32.160 W; Moffa Sanchez et al., 2014). The correlations were calculated over three intervals, the entire time period common to both records (1012-1793 CE) and over the Medieval Climate Anomaly (950 to 1250 CE, MCA) and Little Ice Age (1450 to 1850 CE, LIA). Given the subpolar gyre SSTs were derived from a sedimentary record with decadal temporal resolution (rather than annual), correlations were calculated using 10-year first order loess low pass filtered $\delta^{13}\text{C}$ -shell data. The influence of autocorrelation, which is greater in smoothed time series, was taken into account when calculating the significance of the correlation analyses by using the Ebisuzaki Monte Carlo methodology (Ebisuzaki 1997).

Multiple linear regression model analyses were used to evaluate the long-term stability of the combined influence of the environmental variables identified between the $\delta^{13}\text{C}$ -shell record and the instrumental records. The models were calculated using the reconstructed subpolar gyre SSTs (RAPiD-17-5P data; Moffa Sanchez et al., 2014), the $\delta^{18}\text{O}$ -shell data (Reynolds et al., 2016) and wNAO indexes (Trouet et al., 2009; Ortega et al., 2015). The analyses were performed using R-statistics version 3.4.1 over the entire last millennium and over both the MCA and LIA periods.

3. Results

3.1 Uncertainty analysis

As expected, examination of SE against sample depth (number of shells) of the ontogenetically aligned $\delta^{13}\text{C}$ -shell data (Figure 2) indicates that SE falls as sample depth increases. The SE stabilises at an SE $\leq 0.1\%$ at a sample depth greater than eight shells. Given that sample depth falls with shell longevity, the ontogenetically aligned $\delta^{13}\text{C}$ -shell data are representative of the population $\delta^{13}\text{C}$ -shell variability over the first 45 years of shell growth. The reduction in sample depth after 45 years of growth indicates that variability in the population $\delta^{13}\text{C}$ curve is likely not suitable for ontogenetic analysis after 45 years of age due to the increased influence of variability from individual shells.

The ontogenetically aligned $\delta^{13}\text{C}$ -shell data exhibit variable trends over the first 45 years of shell growth (Figure 2). Examination of the first differential of the low pass filtered ontogenetically aligned $\delta^{13}\text{C}$ data (Figure 2E) identifies three distinct intervals. The first interval, spanning the first 11 years of shell growth, is defined as a period where the first differential is persistently positive. This trend reflects the increase in the mean $\delta^{13}\text{C}$ from the first year of growth until the asymptote is reached at ~ 11 years of age. From the age of 11 to 27 years the first differential is persistently negative, although there is some inter-annual-to-decadal variability. This trend reflects a persistent reduction in mean $\delta^{13}\text{C}$ -shell. After the age of 27 the first differential fluctuates around a mean of zero indicating no persistent trend in the $\delta^{13}\text{C}$ -shell data. Over the first 11 years of shell growth the $\delta^{13}\text{C}$ -shell data exhibit a positive trend equivalent to $0.045 \pm 0.013\% \text{yr}^{-1}$ followed by a trend of $-0.016 \pm 0.006\% \text{yr}^{-1}$ between 11 and 27 years. After the first 27 years of growth there appears to be no statistically significant trend in the ontogenetically aligned $\delta^{13}\text{C}$ -shell data. Based on the empirical determination of these three distinct intervals, linear regression analyses were independently conducted on each section of the $\delta^{13}\text{C}$ -shell data (i.e. 1-11 years, 12-27 years and 28-45 years). Analysis of the $\delta^{13}\text{C}$ -shell data against ontogenetic age (Figure 2) indicates that the trends identified by examination of the first order differential over the first two sections (1-11 and 12-27 years) are highly robust ($R^2=0.98$ and 0.42 respectively $P<0.001$). However, no statistically significant trend was identified over the third period (28-45 years).

The mean standard deviation of the replicate samples analysed in the construction of the complete $\delta^{13}\text{C}$ -shell series is $\pm 0.22\%$ ($\pm 1\sigma$). This value incorporates all the replicate samples, including samples drilled

from the same calendar year in the same shell and in different shells, and the replicate analysis of the same sample. This uncertainty also includes the effects of the ontogenetic vital effects given that the extension of the record required splicing from one shell to the next and this results in $\delta^{13}\text{C}$ -shell values from the ontogenetically youngest portion of a shell being compared with the oldest portion of the next shell in the series. Taken together the replicate sample uncertainty and the analytical uncertainty ($\pm 0.05\text{‰}$) give a total combined root mean squared uncertainty of the $\delta^{13}\text{C}$ -shell of $\sim \pm 0.23\text{‰}$.

3.2 The $\delta^{13}\text{C}$ -shell series

In total, the $\delta^{13}\text{C}$ -shell series contains 1492 annually resolved samples drilled from 21 individual shells spanning the interval from AD 953-2000 (Figure 3). The $\delta^{13}\text{C}$ -shell series has a mean of 2.05‰ (± 0.32 , 1σ). Since the onset of the industrial period (~ 1750 CE) the $\delta^{13}\text{C}$ -shell record contains a negative trend ($-0.003 \pm 0.002\text{‰yr}^{-1}$) whilst over the pre-industrial period the $\delta^{13}\text{C}$ -shell record contains a negligible linear trend of $0.0001 \pm 0.0001\text{‰yr}^{-1}$. Analysis of the fifty-year binned $\delta^{13}\text{C}$ -shell data (Figure 3B) indicates, despite containing a negligible, non-significant, longer-term linear trend, there is significant variability over the pre-industrial era. In total nine of the 50 year bins over the pre-industrial period contain mean $\delta^{13}\text{C}$ -shell values that are either significantly higher or lower than the series mean ($P < 0.05$). Six of these nine bins occur over the interval from 1201-1451 CE. The periods from 1051-1150 CE and 1701-1750 CE account for the other three bins that significantly differ from the series mean. Over the industrial era (1750-2000 CE) four out of five 50 year bins are significantly different to the series mean, with the interval from 1801-1900 CE being significantly more positive ($T = 5.87$ and 9.62 , $P < 0.001$ for the 1801-1850 and 1851-1900 CE respectively) and the period from 1901-2000 CE being significantly lower ($T = -9.228$ and -8.736 , $P < 0.001$ for the 1901-1950 CE and 1951-2000 CE periods respectively). The mean $\delta^{13}\text{C}$ -shell ratio over the period from 1951-2000 CE is statistically different ($P < 0.001$) to the majority of the last 1000 years with the exception of the intervals from 1051-1100 CE, 1351-1400 CE and 1901-1950 CE.

Comparison of the trends contained in the $\delta^{13}\text{C}$ -shell series over recent centuries with other contemporaneous proxies from the North Atlantic Ocean region highlights differences in the amplitudes of variability over different timescales (Figure 3F and Table 1). Examination of the linear trends over the 20th century indicate that the $\delta^{13}\text{C}$ -shell series shifts by $-0.003 \pm 0.002\text{‰yr}^{-1}$ notably less than the trends in previously published *A. islandica* records from Icelandic waters of $-0.013 \pm 0.001\text{‰yr}^{-1}$ (Schöne et al., 2011), the Gulf of Maine ($-0.007 \pm 0.0015\text{‰yr}^{-1}$ (Wanamaker et al., 2008b) and *A. islandica* and sclerosponges from the wider North Atlantic (mean trend $-0.008 \pm 0.002\text{‰yr}^{-1}$, see table 1 for individual records). However, shorter-term trends in $\delta^{13}\text{C}$ -shell series during the period 1979-1999 CE are in strong agreement with a North Atlantic observational time series of $\delta^{13}\text{C}_{\text{DIC}}$ (Schöne et al., 2011; see Table 1).

The MTM spectral analyses identifies significant ($P < 0.1$ to $P < 0.05$; Figure 4; Table 2) sub-decadal (periods of \sim four to eight years) and a centennial (period of ~ 120 years; $P < 0.05$) scale variability in the $\delta^{13}\text{C}$ -shell record (Figure 4A). Wavelet analyses indicates the decadal and centennial scale variability is relatively stable over the last millennium (Figure 4B). However, the wavelet analysis indicates the presence of significant multi-decadal (periods ≥ 20 years) scale variability over portions of the last millennium most notably from ~ 1000 -1450 CE ($P < 0.05$; Figure 4B). The wavelet analyses indicates however that this multi-decadal scale variability is not stable with the period from 1450-1850 CE showing reduced variability at multi-decadal timescales compared to the earlier portion of the record.

3.3 Environmental analyses

Linear regression analyses identify significant positive correlations between the $\delta^{13}\text{C}$ -shell_{detrend} and the offshore North Icelandic shelf phytoplankton productivity record over the period from 1958-1985 CE ($R=0.42$ $P=0.053$). Comparison of the $\delta^{13}\text{C}$ -shell_{detrend} record with onshore phytoplankton productivity on the North Icelandic shelf identified no significant correlation ($R=0.14$, $P=0.52$).

Examination of the coherence between the $\delta^{13}\text{C}$ -shell_{detrend} and detrended instrumental datasets over the 20th century identified a range of significant correlations with different climate variables (Figure 5 and 6). The $\delta^{13}\text{C}$ -shell_{detrend} time series is significantly positively correlated ($P<0.1$) with detrended SSTs (HadISST1; Rayner et al., 2003) over two main geographical regions: (1) the northern limb of the subpolar gyre and (2) the central Equatorial Atlantic (Figure 5A). Significant positive correlations ($P<0.1$) were identified between the $\delta^{13}\text{C}$ -shell_{detrend} and detrended SSSs (UKMO EN4) in geographical regions corresponding to the northern limb of the subpolar gyre and northern stretches of the North Atlantic Current from the northern British Isles to Norway (Figure 5B). Additionally, significant positive correlations were identified between the $\delta^{13}\text{C}$ -shell_{detrend} data and detrended sea ice extent along the east coast of Greenland ($P<0.1$; Figure 5C). The spatial correlation analyses identified significant correlations between the $\delta^{13}\text{C}$ -shell_{detrend} data and detrended SLPs over the North Atlantic with significant positive and negative correlations identified respectively over the Greenland/Iceland and central tropical Atlantic region broadly from the east coast of Africa across to the east coast of Central and South America (Figure 5D). This spatial pattern is characteristic of the dipole in SLPs associated with a negative phase of the wNAO.

Lead-lag analysis indicated the peak correlation between the $\delta^{13}\text{C}$ -shell_{detrend} and detrended annual SSTs (HadISSTs) in the Irminger Current south of Iceland (over the region 55-65°N by 15-25°W) occurs at zero years lag ($R=0.36$, $P<0.05$; Figure 6). However, the peak correlation of the $\delta^{13}\text{C}$ -shell_{detrend} with mean SSS over the same region (55-65°N by 15-25°W) and the wNAO occurs with the $\delta^{13}\text{C}$ -shell_{detrend} series lagging by one year ($R=0.36$, $R=-0.28$ for SSS and wNAO respectively $P<0.05$; Figure 6). The lead-lag analyses identified a complex array of correlations between the $\delta^{13}\text{C}$ -shell_{detrend} series and sea ice extent in the East Greenland Sea (70-80°N by 17-25°W). The strongest correlation was found with the sea ice index lagging by 17 years ($R=-0.31$, $P<0.05$), however, significant correlations were also identified with the sea ice index lagging the $\delta^{13}\text{C}$ -shell_{detrend} series by 2 years ($R=0.23$, $P<0.1$) and the sea ice index leading the $\delta^{13}\text{C}$ -shell_{detrend} series by 10 years ($R=0.27$, $P<0.1$; Figure 6E and I).

A multiple linear regression model was used to examine the cumulative effect of SST, SSS and WNAO variability on phytoplankton productivity on the North Icelandic Shelf. The multiple linear regression model identified that the combined influence of SSTs, SSS, and the wNAO have a significant influence on the $\delta^{13}\text{C}$ -shell_{detrend} (multiple- $R^2=0.24$, $F=10.3$, $P<0.001$). These analyses indicate that whilst each of the individual parameters explain a relatively small degree (8-13%) of variability in the $\delta^{13}\text{C}$ -shell_{detrend} series, they combine to explain a larger degree (24%) of the variance in the annually resolved multi-decadal scale $\delta^{13}\text{C}$ -shell_{detrend} variability.

Comparison of the $\delta^{13}\text{C}$ -shell data against contemporary proxies yielded varied results (Figure 7). No significant correlation was found between the $\delta^{13}\text{C}$ -shell data and North Icelandic shelf ΔR (Wanamaker et al., 2012; $R=-0.03$, $P>0.1$, $N=31$). Additionally, no significant correlation was found between the $\delta^{18}\text{O}$ -shell (Reynolds et al., 2016) and the $\delta^{13}\text{C}$ -shell records at annual resolution ($R=-0.12$, $P=0.15$). However, examination of the 100-year running correlations, calculated using both the annually resolved data and 100-year high pass filtered data, indicated persistent periods characterised by significant

negative correlations ($R=-0.20$, $P<0.1$, significance level calculated using the Ebisuzaki Monte Carlo methodology) interrupted by excursions towards positive correlations most notably over the period between 1570-1750 CE ($R=0.34$, $P<0.01$). Comparison between the 100-year high pass filtered $\delta^{13}\text{C}$ -shell_{detrend} data and the RCS chronology (Butler et al., 2013) indicated a significant, albeit weak, correlation ($R=0.10$, $P<0.05$). Correlation coefficients calculated between the $\delta^{13}\text{C}$ -shell data and wNAO indexes (Trouet et al., 2009, Ortega et al., 2015) indicate no significant relationship over the entire record. However, as with the oxygen isotopes, examination of the running correlation coefficients indicates that over the period 1400-1700 CE the $\delta^{13}\text{C}$ -shell data correlates significantly with both wNAO indexes ($R=-0.24$ and -0.16 , $P<0.1$ at annual resolution and $R=-0.50$ and -0.55 $P<0.05$ with the 30-year low pass filtered data respectively). Over the period 1000-1400 CE however the $\delta^{13}\text{C}$ -shell data contains a significant positive correlation with the Trouet et al. (2009) data ($R=0.43$ and 0.57 , $P<0.5$ at annual resolution and 30 year low pass filtered respectively). The correlation with the Ortega et al. (2015) wNAO index also exhibits a shift towards positive correlations, however the correlation over the 1000-1400 CE period is not significant ($R=0.18$ and 0.30 $P>0.1$ at annual resolution and 30-year low pass filtered respectively).

Linear regression analyses between 10-year first order loess low pass filtered $\delta^{13}\text{C}$ -shell_{detrended} and subpolar gyre SSTs recorded in core RAPID-17-5P identified a significant negative correlation over the contemporaneous sampling period 1012-1793 CE ($R=-0.26$ $P=0.05$). The relationship over the MCA interval (1012-1400 CE) indicated a strengthened significant correlation ($R=-0.47$, $P<0.05$) whilst over the LIA (1400-1793 CE) the series exhibited a non-significant correlation ($R=0.18$ $P>0.1$). Correlation between the 10-year first order loess low pass filtered $\delta^{18}\text{O}$ -shell record and subpolar gyre SSTs indicated a significant negative correlation ($R=-0.27$, $P<0.05$), calculated over the period 1012-1793 CE. As with the $\delta^{13}\text{C}$ -shell_{detrended} data, the strength of the correlation was increased over the MCA period ($R=-0.36$ $P<0.05$), whilst no significant correlations were identified over the LIA ($R=-0.12$, $P>0.1$).

The multiple linear regression model indicates that over the entire last millennium, using available comparable proxy records, the combined influence of the subpolar gyre SSTs (Moffa Sanchez et al., 2012) and the wNAO (using either the Trouet et al., 2009 or the Ortega et al., 2015 wNAO reconstructions) explains 9% of the variability in the 10-year low pass filtered $\delta^{13}\text{C}$ -shell_{detrended} record. However, over the MCA period (1000-1400) the percentage variance explained by these proxy records increases to 25% and 37% (using the Ortega et al., 2015 and Trouet et al., 2009 wNAO reconstructions respectively; $P<0.001$). Incorporating the $\delta^{18}\text{O}$ -shell record into the model, in addition to the wNAO and subpolar gyre SSTs, did not change the percentage of variance explained over either the entire last millennium or the MCA time intervals. Over the LIA (1400-1800 CE) the multiple linear regression model indicates that subpolar gyre SSTs and the wNAO explains 11% and 16% of the variance in the $\delta^{13}\text{C}$ -shell record (using the Ortega et al., 2015 and Trouet et al., 2009 wNAO reconstructions respectively; $P<0.001$). Incorporating the $\delta^{18}\text{O}$ -shell data into the model increases the R^2 value to 22% ($P<0.001$) for both the Ortega et al., (2015) and Trouet et al., (2009) based wNAO reconstructions. Excluding the subpolar gyre SSTs from the model results in the multiple linear regression model explaining 20% and 22% of the variance in the $\delta^{13}\text{C}$ -shell_{detrended} record using the Ortega et al. (2015) and Trouet et al. (2009) based reconstructions respectively.

4. Discussion

Our analysis of $\delta^{13}\text{C}$ -shell material from 21 individual shells demonstrates that during the first 27 years of shell growth vital effects significantly influence the $\delta^{13}\text{C}$ -shell composition of *A. islandica* shells.

The ontogenetically aligned $\delta^{13}\text{C}$ -shell data indicate a gradual increase in $\delta^{13}\text{C}$ -shell values over the first 11 years of shell growth followed by a gradual decrease in $\delta^{13}\text{C}$ -shell values between the age of 12 and 27 years. This result is in agreement with previous observations in *A. islandica* shells (Butler et al. 2011). However, while the trend we observe in our $\delta^{13}\text{C}$ -shell records over the first 27 years of growth was significant, there is a large degree of variance evident with biological age in the zero normalised $\delta^{13}\text{C}$ -shell data. This demonstrates that although vital effects contribute to the variability in $\delta^{13}\text{C}$ -shell over the first 27 years, typically creating a positive shift of $\sim 0.1\text{‰}$, the influence is ultimately a small component of the overall variability preserved in the $\delta^{13}\text{C}$ -shell record. Furthermore, the influence of these vital effects is minimised during the construction of the 1000-year $\delta^{13}\text{C}$ -shell record as young biologically aged samples, most strongly influenced by vital effects, typically occur at periods of shell overlap and are therefore averaged with $\delta^{13}\text{C}$ -shell measurements from shells with a biological age not influenced by vital effects during the splicing necessary to extend the record beyond the lifespan of one individual.

The $\delta^{13}\text{C}$ -shell record presented here represents the first continuous, well-replicated, annually resolved record of marine $\delta^{13}\text{C}_{\text{DIC}}$ that spans the entire last millennium. The $\delta^{13}\text{C}$ -shell record contains both similarities with, and differences to, contemporaneous records of marine and atmospheric $\delta^{13}\text{C}$. The general trend contained in the $\delta^{13}\text{C}$ -shell record shows a stable mean over the pre-industrial period followed by an exponential decline to lower values over the industrial period consistent with atmospheric $\delta^{13}\text{C}$ recorded in Antarctic ice cores (see Figure 3C, data from Francey et al., 1999), tropical Atlantic marine $\delta^{13}\text{C}$ recorded in sclerosponges (Figure 3D; Böhm et al., 2002) and with sub-tropical to subpolar marine $\delta^{13}\text{C}$ reconstructions derived from other *A. islandica* records (Butler et al., 2009, Schöne et al., 2011) that extend over the last ~ 500 years (Figure 3). However, the degree of variability observed during the pre-industrial period in our subpolar $\delta^{13}\text{C}$ -shell record is greater than seen in the sclerosponge record from the tropical Atlantic Ocean (Böhm et al., 2002). Variability in the tropical Atlantic $\delta^{13}\text{C}$ records is typically constrained within $\sim \pm 0.15\text{‰}$ of the mean with the only significant shift occurring over the industrial period due to the influence of the marine Suess effect (Figure 3D). The $\delta^{13}\text{C}$ -shell record however contains significant variability over the pre-industrial era with the analysis of the 50-year bins indicating several periods which significantly ($P < 0.05$) differ (both positive and negative shifts) from the long-term mean. The greatest period of variability occurs over the interval between 1201 - 1451 CE that contain six consecutive 50-year bins that are significantly different from the series mean. This interval, which broadly coincides with the transition between the MCA and the LIA, is characterised by significant oceanographic and climatic changes on the North Icelandic Shelf (Wanamaker et al., 2012, Reynolds et al., 2016).

The comparison of the extent of the marine Suess effect in the $\delta^{13}\text{C}$ -shell record and contemporaneous $\delta^{13}\text{C}$ proxy records from the wider North Atlantic region indicates that the $\delta^{13}\text{C}$ -shell record contains an attenuated Suess effect ($-0.003 \pm 0.002\text{‰yr}^{-1}$) compared with other proxy records (mean Suess effect of the contemporaneous proxies $-0.009 \pm 0.003\text{‰yr}^{-1}$; Table 1). The $\delta^{13}\text{C}$ records derived from *A. islandica* shells from shallower North Icelandic coastal waters indicate that the attenuated response to the marine Suess effect signal is unique to the $\delta^{13}\text{C}$ -shell record, with the shallow North Icelandic records containing a mean trend of $-0.013 \pm 0.001\text{‰yr}^{-1}$ (Schöne et al., 2011). The attenuated response of marine carbon records at 80m water depth on the North Icelandic shelf has been identified previously through the examination of radiocarbon (^{14}C) bomb-pulse records (Scourse et al., 2012). The marine bomb-pulse curve, which was generated using the same shells used to construct the $\delta^{13}\text{C}$ -shell record, contains a significantly attenuated ^{14}C signal with respect to bomb-pulse curves generated from the wider North Atlantic environment (Norwegian Sea, North Sea, and the Gulf of Maine) and the

atmosphere (Scourse et al., 2012). Examination of short term trends in the $\delta^{13}\text{C}$ -shell record against an observational index of North Atlantic $\delta^{13}\text{C}_{\text{DIC}}$ (Schöne et al., 2011) indicates that on decadal timescales shifts in the $\delta^{13}\text{C}$ -shell record match those of the wider North Atlantic ($-0.039 \pm 0.01\text{‰yr}^{-1}$ and $-0.039 \pm 0.05\text{‰yr}^{-1}$ for the North Atlantic $\delta^{13}\text{C}_{\text{DIC}}$ and $\delta^{13}\text{C}$ -shell records respectively; Table 1). These results could indicate that the processes that lead to the attenuation of the long-term trends in $\delta^{13}\text{C}_{\text{DIC}}$ at 80 m water depth on the North Icelandic shelf may have a greater influence on longer timescales with multi-decadal variability being reflected in the $\delta^{13}\text{C}$ -shell record.

An examination of the spatial correlations between the $\delta^{13}\text{C}$ -shell_{detrend} and linearly detrended instrumental data (SST, SSS and SLP) indicates significant links between $\delta^{13}\text{C}_{\text{DIC}}$ and climate variability over the 20th century (Figures 5 and 6). In particular, the spatial correlations indicate that SST and SSS variability in the northern limb of the subpolar gyre and shifts in atmospheric circulation patterns associated with the wNAO are the likely physical mechanisms that influence variability in the North Icelandic shelf $\delta^{13}\text{C}$ -shell_{detrend} record. The spatial extent of the $\delta^{13}\text{C}$ -shell_{detrend} correlations with SST and SSS are mainly south of Iceland (Figure 5) strongly suggesting that the influence of varying SST and SSS is associated with the advection of SPMW from the northern limb of the subpolar gyre, via the Irminger Current, onto the North Icelandic shelf. Over the 20th century records show that shifts in the relative proportion of SPMW and AIW on the North Icelandic shelf have led to pronounced changes in the rate of primary production in this region (Gudmundsson, 1998). Given the significant correlation between offshore phytoplankton productivity and the $\delta^{13}\text{C}$ -shell_{detrend} record ($R=0.42$ $P=0.053$) it could be hypothesised that primary production variability is a key driver of $\delta^{13}\text{C}_{\text{DIC}}$ on the North Icelandic shelf. In addition to the coherence with SST and SSS, the spatial correlation analyses indicate that SLP variability correlates significantly with the $\delta^{13}\text{C}$ -shell_{detrend} (Figures 5 and 6). Changes in atmospheric circulation patterns, associated with wNAO, drive changes in wind strength and direction over the North Atlantic. On a regional scale, changing wind strength and direction leads to changes in the strength and depth of mixing in the water column and the advection of SPMW onto the North Icelandic shelf that in turn influences rates of primary production. The wNAO is also associated with the strength of the subpolar gyre, with positive phases of the wNAO generally being associated with a strong subpolar gyre circulation coupled with negative SST anomalies in the central subpolar gyre region (Moffa-Sánchez et al., 2014). The positive correlation between the $\delta^{13}\text{C}$ -shell_{detrend} record and instrumental SSTs from the northern limb of the subpolar gyre (Figure 5) indicates that the reduction in SSTs is then propagated through the Irminger Current onto the North Icelandic shelf leading to a reduction in primary production. The negative correlation between the $\delta^{13}\text{C}$ -shell series and wNAO proxy series, evident over the Little Ice Age and with instrumental observations, suggests that the influence of variable SPMW advection to the North Icelandic shelf has persisted since the onset of the LIA, a period characterised by reduced SPMW on the North Icelandic shelf (Wanamaker et al., 2012). Over the MCA period, where proxy evidence suggests a greater proportion of SPMW was entrained onto the North Icelandic shelf (Wanamaker et al., 2012, Reynolds et al., 2016), the $\delta^{13}\text{C}$ -shell series and wNAO proxy series show significant and non-significant positive correlations with the Trouet et al. (2009) and Ortega et al. (2015) reconstructions respectively. The non-stationary relationship between the wNAO and SSTs has been shown in observational records (Polyakova et al., 2006). Over the modern instrumental period it has been shown that when SSTs are typically warm (cold) in the North Atlantic SSTs correlate positively (negatively) with the wNAO (Polyakova et al., 2006). Polyakova et al. (2006) hypothesise that the variability in sign of the correlation between SSTs and the wNAO is likely non-random and driven by physical mechanisms across the subpolar North Atlantic region. The significant switch in sign of the correlation between the $\delta^{13}\text{C}$ -shell_{detrend} series and the wNAO between the MCA and LIA periods,

during which there were contemporaneous shifts in the oceanographic regime on the north Icelandic shelf, would appear to support this hypothesis.

During the MCA interval both the $\delta^{13}\text{C}$ -shell_{detrend} and $\delta^{18}\text{O}$ -shell records exhibit strong significant correlations with reconstructed subpolar gyre SWTs (Moffa Sanchez et al., 2012; $R=-0.47$ and -0.36 respectively; $P<0.05$). In contrast during the LIA, where it is hypothesised that there was reduced entrainment of AIW onto the North Icelandic shelf (Wanamaker et al., 2012), the coherence between the $\delta^{13}\text{C}$ -shell_{detrend} and $\delta^{18}\text{O}$ -shell records with subpolar gyre SSTs is reduced ($R=0.18$ and -0.12 ; $P>0.1$ respectively). The pattern of shifting coherence between the variability on the North Icelandic shelf and that of the subpolar gyre between the MCA and the LIA supports the hypothesis that during the MCA (LIA) a greater (lesser) proportion of SPMW was entrained onto the North Icelandic shelf.

Numerous proxy-based reconstructions indicate significant long-term climatic variability in the subpolar North Atlantic region over the last millennium that is broadly characterised as a transition from a warm MCA into a cooler LIA (Sicre et al., 2008, Sejrup et al., 2010, Wanamaker et al., 2012, Cunningham et al., 2013, Halfar et al., 2013, Moffa-Sánchez et al., 2014, Reynolds et al., 2016). Given the sensitivity of the $\delta^{13}\text{C}$ -shell record to environmental variability over the 20th century it might be expected that the $\delta^{13}\text{C}$ -shell series would contain similar long-term trends. Such a long-term shift would also be suspected if the hypothesis holds that there was a reduction in the proportion of SPMW on the North Icelandic shelf between the MCA and LIA given the observed differences in $\delta^{13}\text{C}_{\text{DIC}}$ between modern mean annual surface SPMW and AIW are $\sim 0.6\text{‰}$ (Tagliabue and Bopp, 2008, Olsen and Ninnemann, 2010). However, the $\delta^{13}\text{C}$ -shell contains no long-term linear trend over the pre-industrial era. The lack of a long-term trend during the pre-industrial era suggests either that there is no shift in $\delta^{13}\text{C}_{\text{DIC}}$ (and therefore, by extension, primary production or water mass composition) on the North Icelandic shelf or that any shift in $\delta^{13}\text{C}_{\text{DIC}}$ as a result of a change in primary production or water mass composition is being offset by other factors at this locality (e.g. changes in air-sea CO_2 exchange, deep water mixing onto the shelf; Lynch-stieglitz et al., 1995; Zeebe and Wolf-Gladrow, 2001).

The hypothesis that contrasting $\delta^{13}\text{C}$ fractionation mechanisms likely mitigate the local $\delta^{13}\text{C}_{\text{DIC}}$ response to long-term shifts in climate over the pre-industrial era may also explain the attenuated marine Suess effect captured by our $\delta^{13}\text{C}$ -shell record and the reduced amplitude of the marine radiocarbon bomb pulse at this locality, recorded by the same shells (Scourse et al., 2012). The strength of the marine Suess effect signal is strongly linked to the degree in which the source waters are equilibrated with the atmosphere (Eide et al., 2017). As such, there can be considerable differences between the amplitude of the marine Suess effect between water masses and with increasing water depth (Eide et al., 2017). As has been shown with the North Icelandic ΔR record, AIW source waters have a relatively older ΔR age than SPMW due to AIW being less equilibrated with the atmosphere than SPMW (Wanamaker et al., 2012). The reduced level of equilibrium with the atmosphere would therefore lead to a reduced marine Suess effect signal in *A. islandica* shells living in AIW source waters. In addition, there is a direct difference in the $\delta^{13}\text{C}_{\text{DIC}}$ composition of SPMW and AIW of $\sim 0.6\text{‰}$, with typical modern SPMW and AIW $\delta^{13}\text{C}_{\text{DIC}}$ values of $\sim 1.4\text{‰}$ and 2.0‰ respectively (Tagliabue and Bopp, 2008, Olsen and Ninnemann, 2010). Shifts in the relative proportion of SPMW and AIW entrained onto the North Icelandic shelf could therefore lead to significant shifts in $\delta^{13}\text{C}_{\text{DIC}}$ that could mask the long-term marine Suess effect signal. Examination of the North Icelandic shelf ΔR series (Wanamaker et al., 2012) over the period from 1700-1950 CE (Figure 7E) and instrumental observations (Dickson et al., 1996, Dickson et al., 1988, Hanna et al., 2004), suggests that over the industrial period there has been significant variability in the water mass composition on the North Icelandic shelf. These shifts in water

mass between periods characterised by AIW to SPMW dominance would bring about large shifts in $\delta^{13}\text{C}_{\text{DIC}}$ of up to 0.6‰, assuming there are no other corresponding changes in $\delta^{13}\text{C}_{\text{DIC}}$ due to, for example, primary production. The general recent trend has been towards a shift away from AIW towards SPMW, that could explain why in the later decades of the 20th century the $\delta^{13}\text{C}$ -shell record more closely reflects wider changes in North Atlantic $\delta^{13}\text{C}_{\text{DIC}}$. In addition to these long-term changes, significant variability in water mass composition has been observed over the instrumental period (e.g. the great salinity anomaly; Dickson et al., 1996, Dickson et al., 1988, Hanna et al., 2004). These shifts in water mass would also have implications for primary production dynamics. Primary production in Icelandic waters is largely controlled by sea surface salinity variability and the stability of the water column (Gudmundsson, 1998). In addition to differences in total phytoplankton productivity, SPMW and AIWs contain different seasonal primary production signatures. SPMW primary production is characterised by several peaks occurring throughout the year. In contrast primary production in AIWs is characterised by a single peak in phytoplankton productivity in late March to early May coinciding with the onset of *A. islandica* shell growth in this region (Gudmundsson, 1998). Given the salinity and temperature differences between SPMW and AIW it is not surprising there are observable differences between the overall level and the seasonal structure of primary production between AIW and SPMW waters across the Icelandic shelf seas (Gudmundsson, 1998). These shifts in production that would occur over both short and long-timescales in response to shifts in water mass dynamics and wider climate variability would also add significant variability that could result in divergence from the long-term atmospheric $\delta^{13}\text{C}$ signal.

Differences between the new $\delta^{13}\text{C}$ -shell record presented here and other North Icelandic $\delta^{13}\text{C}$ -shell records (e.g. Schöne et al., 2011) can be reconciled by differences in the water depth from where the shells were collected. Over the observational period it has been shown that the strength of the marine Suess effect signal is driven in part by water depth (Eide et al., 2017). It is therefore unsurprising that the Schöne et al. (2011) study, that investigated shell material collected from shallow water environments, reports a strengthened marine Suess effect relative to that captured by the new $\delta^{13}\text{C}$ -shell record. Similar reduced amplitude variability has been observed in the radiocarbon bomb pulse signals captured by the *A. islandica* collected at 80 m water depth on the North Icelandic shelf (Scourse et al., 2012). For instance, whilst the North Icelandic shells exhibit a relatively low amplitude bomb pulse, records from temperate Atlantic shelf seas (e.g. the North Sea and the Sea of the Hebrides) contain relatively enhanced ^{14}C concentrations relative to records from relatively more polar settings (Scourse et al., 2012, Reynolds et al., 2013).

5. Conclusions

The new 1000 year $\delta^{13}\text{C}$ -shell record from the North Icelandic shelf demonstrates that it is possible to generate robust long-term absolutely dated baselines of marine $\delta^{13}\text{C}$ variability by examining the stable isotopic composition of *A. islandica* shells. The record contained in the $\delta^{13}\text{C}$ -shell archive indicates there has been considerable multi-decadal scale variability in marine $\delta^{13}\text{C}_{\text{DIC}}$ on the North Icelandic shelf over the last 1000 years. The most significant shift in the $\delta^{13}\text{C}$ -shell record results from the marine ^{13}C Suess effect. The analyses of the $\delta^{13}\text{C}$ -shell record against a range of instrumental climate-related observations indicates that climate variability has played a significant role in driving marine $\delta^{13}\text{C}$ variability over the 20th century and likely over the last millennium. The utilisation of a multi-sclerochronological proxy based approach may allow for the removal of primary production induced $\delta^{13}\text{C}$ variability from the $\delta^{13}\text{C}$ -shell record facilitating a closer examination of the oceanographic and air-sea CO_2 fractionation based variability. The utilisation of these techniques in areas that are not dominated by water mass dynamics could enable the direct reconstruction of air-sea CO_2 flux at annual

resolution over past centuries. Given the significant, yet variable, role the North Atlantic plays as a net sink in the global carbon cycle, the ability to quantify the mechanisms and uncertainties surrounding this carbon sink will play an important part in constraining future projections of marine and atmospheric CO₂ dynamics.

Acknowledgements

We thank the members of the RV *Bjarni Sæmundsson* (Cruise No. B05-2006). This work was supported by the NERC-funded ULTRA project (Grant Number NE/H023356/1), NERC-funded CLAM project (Project No. NE/N001176/1) and EU Millennium Project (Project number 017008). This study is a contribution to the Climate Change Consortium for Wales (C3W). We thank Brian Long (Bangor University) and Dr Julia Becker (Cardiff University) for their technical support. We would like to thank the two anonymous reviewers for their constructive comments and recommendations.

Data availability

The $\delta^{13}\text{C}$ -shell data are available from the NOAA palaeo data archive <https://www.ncdc.noaa.gov/paleo/study/22950>

References

- Allan, R. & Ansell, T. (2006). A new globally complete monthly historical gridded mean sea level pressure dataset (HadSLP2): 1850-2004. *Journal of Climate*, 19, 5816-5842.
- Beirne, E. C., Wanamaker, A. D., Jr. & Feindel, S. C. (2012). Experimental validation of environmental controls on the delta C-13 of *Arctica islandica* (ocean quahog) shell carbonate. *Geochimica Et Cosmochimica Acta*, 84, 395-409.
- Bohm, F., Haase-Schramm, A., Eisenhauer, A., Dullo, W. C., Joachimski, M. M., Lehnert, H. & Reitner, J. (2002). Evidence for preindustrial variations in the marine surface water carbonate system from coralline sponges. *Geochemistry Geophysics Geosystems*, 3.
- Bohm, F., Joachimski, M. M., Lehnert, H., Morgenroth, G., Kretschmer, W., Vacelet, J. & Dullo, W. C. (1996). Carbon isotope records from extant Caribbean and south Pacific sponges: Evolution of delta C-13 in surface water DIC. *Earth and Planetary Science Letters*, 139, 291-303.
- Broecker, W. S. & Peng, T. H. (1974). Gas-exchange rates between air and sea. *Tellus*, 26, 21-35.
- Butler, P. G., Scourse, J. D., Richardson, C. A., Wanamaker Jr, A. D., Bryant, C. L. & Bennell, J. D. (2009). Continuous marine radiocarbon reservoir calibration and the ^{13}C Suess effect in the Irish Sea: Results from the first multi-centennial shell-based marine master chronology. *Earth and Planetary Science Letters*, 279, 230-241.
- Butler, P. G., Wanamaker, A. D., Jr., Scourse, J. D., Richardson, C. A. & Reynolds, D. J. (2011). Long-term stability of delta C-13 with respect to biological age in the aragonite shell of mature specimens of the bivalve mollusk *Arctica islandica*. *Palaeogeography Palaeoclimatology Palaeoecology*, 302, 21-30.
- Butler, P. G., Wanamaker, A. D., Scourse, J. D., Richardson, C. A. & Reynolds, D. J. (2013). Variability of marine climate on the North Icelandic Shelf in a 1357-year proxy archive based on growth

682 increments in the bivalve *Arctica islandica*~ *Palaeogeography, Palaeoclimatology, Palaeoecology*,
683 373, 141-151.

684 Cage, A. G. & Austin, W. E. N. (2010). Marine climate variability during the last millennium: The Loch
685 Sunart record, Scotland, UK. *Quaternary Science Reviews*, 29, 1633-1647.

686 Conway, T. J., Tans, P. P., Waterman, L. S. & Thoning, K. W. (1994). Evidence for interannual
687 variability of the carbon-cycle from the national-oceanic-and-atmospheric-administration
688 climate-monitoring-and-diagnostics-laboratory global-air-sampling-network. *Journal of*
689 *Geophysical Research-Atmospheres*, 99, 22831-22855.

690 Cunningham, L. K., Austin, W. E., Knudsen, K. L., Eiriksson, J., Scourse, J. D., Wanamaker, A. D.,
691 Butler, P. G., Cage, A. G., Richter, T., Husum, K., Hald, M., Andersson, C., Zorita, E.,
692 Linderholm, H. W., Gunnarson, B. E., Sicre, M. A., Sejrup, H. P., Jiang, H. & Wilson, R. J.
693 (2013). Reconstructions of surface ocean conditions from the northeast Atlantic and Nordic
694 seas during the last millennium. *The Holocene*, 23, 921-935.

695 Dickson, R., J. Lazier, J. Meincke, P. Rhines and J. Swift (1996). Long-term coordinated changes in
696 the convective activity of the north atlantic. *Progress in Oceanography*, 38, 241-295.

697 Dickson, R. R., J. Meincke, S. A. Malmberg and A. J. Lee (1988). The great salinity anomaly in the
698 northern north-atlantic 1968-1982. *Progress in Oceanography*, 20, 103-151.

699 Degrandpre, M. D., A. Kortzinger, U. Send, D. W. R. Wallace and R. G. J. Bellerby (2006). Uptake
700 and sequestration of atmospheric co₂ in the labrador sea deep convection region. *Geophysical*
701 *Research Letters*, 33.

702 Doney, S. C., Fabry, V. J., Feely, R. A. & Kleypas, J. A. (2009). Ocean Acidification: The Other CO₂
703 Problem. *Annual Review of Marine Science*, 1, 169-192.

704 Ebisuzaki, W. (1997). A method to estimate the statistical significance of a correlation when the data
705 are serially correlated. *Journal of Climate*, 10, 2147-2153.

706 Eide, M., A. Olsen, U. S. Ninnemann & Eldevik T. (2017). A global estimate of the full oceanic c-13
707 suess effect since the preindustrial. *Global Biogeochemical Cycles*, 31, 492-514.

708 Eiriksson, J., Knudsen, K. L., Larsen, G., Olsen, J., Heinemeier, J., Bartels-Jonsdottir, H. B., Jiang, H.,
709 Ran, L. & Simonarson, L. A. (2011). Coupling of palaeoceanographic shifts and changes in
710 marine reservoir ages off North Iceland through the last millennium. *Palaeogeography*
711 *Palaeoclimatology Palaeoecology*, 302, 95-108.

712 Francey, R. J., Allison, C. E., Etheridge, D. M., Trudinger, C. M., Enting, I. G., Leuenberger, M.,
713 Langenfelds, R. L., Michel, E. & Steele, L. P. (1999). A 1000-year high precision record of delta
714 C-13 in atmospheric CO₂. *Tellus Series B-Chemical and Physical Meteorology*, 51, 170-193.

715 Galbraith, E. D., Kwon, E. Y., Bianchi, D., Hain, M. P. & Sarmiento, J. L. (2015). The impact of
716 atmospheric pCO₂ on carbon isotope ratios of the atmosphere and ocean. *Global*
717 *Biogeochemical Cycles*, 29, 307-324.

718 Good, S. A., Martin, M. J. & Rayner, N. A. (2013). EN4: Quality controlled ocean temperature and
719 salinity profiles and monthly objective analyses with uncertainty estimates. *Journal of*
720 *Geophysical Research-Oceans*, 118, 6704-6716.

721 Gruber, N., Keeling, C. D., Bacastow, R. B., Guenther, P. R., Lueker, T. J., Wahlen, M., Meijer, H. A.
722 J., Mook, W. G. & Stocker, T. F. (1999). Spatiotemporal patterns of carbon-13 in the global
723 surface oceans and the oceanic Suess effect. *Global Biogeochemical Cycles*, 13, 307-335.

724 Gudmundsson, K. (1998). Long-term variation in phytoplankton productivity during spring in Icelandic
725 waters. *Ices Journal of Marine Science*, 55, 635-643.

726 Halfar, J., Adey, W. H., Kronz, A., Hetzinger, S., Edinger, E. & Fitzhugh, W. W. (2013). Arctic sea-
727 ice decline archived by multicentury annual-resolution record from crustose coralline algal proxy.
728 *Proceedings of the National Academy of Sciences of the United States of America*, 110, 19737-
729 19741.

730 Hanna, E., T. Jonsson and J. E. Box (2004). An analysis of icelandic climate since the nineteenth
731 century. *International Journal of Climatology*, 24, 1193-1210.

732 IPCC (2013). *IPCC, 2013: Climate Change 2013: The Physical Science Basis. Contribution of Working*
733 *Group I to the Fifth Assessment Report of the Intergovernmental Panel on Climate Change*,
734 Cambridge University Press, Cambridge, United Kingdom and New York, NY, USA,.

735 Keeling, C. D., Piper, S. C., Bacastow, R. B., Wahlen, M., Whorf, T. P., Heimann, M. & Meijer, H. A.
736 (2005). Atmospheric CO₂ and ¹³CO₂ Exchange with the Terrestrial Biosphere and Oceans from
737 1978 to 2000: Observations and Carbon Cycle Implications. *In*: Baldwin, I. T., Caldwell, M. M.,
738 Heldmaier, G., Jackson, R. B., Lange, O. L., Mooney, H. A., Schulze, E. D., Sommer, U.,
739 Ehleringer, J. R., Denise Dearing, M. & Cerling, T. E. (eds.) *A History of Atmospheric CO₂ and*
740 *Its Effects on Plants, Animals, and Ecosystems*. New York, NY: Springer New York.

741 Logemann, K., Ólafsson, J., Snorrason, Á., Valdimarsson, H. & Marteinsdóttir, G. (2013). The
742 circulation of Icelandic waters – a modelling study. *Ocean Science*, 9, 931-955.

743 Lynch-Stieglitz, J., Stocker, T. F., Broecker, W. S. & Fairbanks, R. G. (1995). The influence of air-sea
744 exchange on the isotopic composition of oceanic carbon - observations and modeling. *Global*
745 *Biogeochemical Cycles*, 9, 653-665.

746 Marchitto, T. M., Jones, G. A., Goodfriend, G. A. & Weidman, C. R. (2000). Precise temporal
747 correlation of holocene mollusk shells using sclerochronology. *Quaternary Research*, 53, 236-
748 246.

749 Mckinley, G. A., Follows, M. J. & Marshall, J. (2004). Mechanisms of air-sea CO₂ flux variability in
750 the equatorial Pacific and the North Atlantic. *Global Biogeochemical Cycles*, 18.

751 Moffa-Sánchez, P., Born, A., Hall, I. R., Thornalley, D. J. R. & Barker, S. (2014). Solar forcing of
752 North Atlantic surface temperature and salinity over the past millennium. *Nature Geoscience*, 7,
753 275-278.

754 Nozaki, Y., Rye, D. M., Turekian, K. K. & Dodge, R. E. (1978). 200-year record of c-13 and c-14
755 variations in a bermuda coral. *Geophysical Research Letters*, 5, 825-828.

756 Olsen, A. & Ninnemann U. (2010). Large delta c-13 gradients in the preindustrial north atlantic
757 revealed. *Science*, 330, 658-659.

758 Ortega, P., Lehner, F., Swingedouw, D., Masson-Delmotte, V., Raible, C. C., Casado, M. & Yiou, P.
759 (2015). A model-tested North Atlantic Oscillation reconstruction for the past millennium. *Nature*,
760 523, 71-+.

761 Peterson, B. J. & Fry, B. (1987). Stable Isotopes In Ecosystem Studies. *Annual Review of Ecology and*
762 *Systematics*, 18, 293-320.

763 Peylin, P., Bousquet, P., Le Quere, C., Sitch, S., Friedlingstein, P., Mckinley, G., Gruber, N., Rayner,
764 P. & Ciais, P. (2005). Multiple constraints on regional CO₂ flux variations over land and oceans.
765 *Global Biogeochemical Cycles*, 19.

766 Polyakova, E. I., Journal, A. G., Polyakov, I. V. & Bhatt, U. S. (2006). Changing relationship between
767 the North Atlantic Oscillation and key North Atlantic climate parameters. *Geophysical Research*
768 *Letters*, 33.

769 Rayner, N. A., Parker, D. E., Horton, E. B., Folland, C. K., Alexander, L. V., Rowell, D. P., Kent, E.
770 C. & Kaplan, A. (2003). Global analyses of sea surface temperature, sea ice, and night marine air
771 temperature since the late nineteenth century. *Journal of Geophysical Research-Atmospheres*,
772 108.

773 Reynolds, D. J., Richardson, C. A., Scourse, J. D., Butler, P. G., Wanamaker, A. D., Ridgway, I., Sayer,
774 M. D. J. & Gulliver, P. (2013). The potential of the marine bivalve mollusc *Glossus humanus*
775 (L.) as a sclerochronological archive. *Holocene*, 23, 1711-1720.

776 Reynolds, D. J., Scourse, J. D., Halloran, P. R., Nederbragt, A. J., Wanamaker, A. D., Butler, P. G.,
777 Richardson, C. A., Heinemeier, J., Eiriksson, J., Knudsen, K. L. & Hall, I. R. (2016). Annually
778 resolved North Atlantic marine climate over the last millennium. *Nature Communications*, 7.

779 Sabine, C. L., Feely, R. A., Gruber, N., Key, R. M., Lee, K., Bullister, J. L., Wanninkhof, R., Wong, C.
780 S., Wallace, D. W. R., Tilbrook, B., Millero, F. J., Peng, T. H., Kozyr, A., Ono, T. & Rios, A. F.
781 (2004). The oceanic sink for anthropogenic CO₂. *Science*, 305, 367-371.

782 Schöne, B. R., Wanamaker, A. D., Jr., Fiebig, J., Thebault, J. & Kreutz, K. (2011). Annually resolved
783 delta C-13(shell) chronologies of long-lived bivalve mollusks (*Arctica islandica*) reveal oceanic
784 carbon dynamics in the temperate North Atlantic during recent centuries. *Palaeogeography*
785 *Palaeoclimatology Palaeoecology*, 302, 31-42.

786 Schöne, B. R., Fiebig, J., Pfeiffer, M., Gless, R., Hickson, J., Johnson, A. L. A., Dreyer, W. &
787 Oschmann, W. (2005). Climate records from a bivalved *Methuselah* (*Arctica islandica*, Mollusca;
788 Iceland). *Palaeogeography Palaeoclimatology Palaeoecology*, 228, 130-148.

789 Schöne, B. R., Wanamaker, A. D., Fiebig, J., Thébault, J. & Kreutz, K. (2011). Annually resolved
790 $\delta^{13}\text{C}_{\text{shell}}$ chronologies of long-lived bivalve mollusks (*Arctica islandica*) reveal oceanic carbon
791 dynamics in the temperate North Atlantic during recent centuries. *Palaeogeography*,
792 *Palaeoclimatology, Palaeoecology*, 302, 31-42.

793 Scourse, J., Richardson, C., Forsythe, G., Harris, I., Heinemeier, J., Fraser, N., Briffa, K. & Jones, P.
794 (2006). First cross-matched floating chronology from the marine fossil record: data from growth
795 lines of the long-lived bivalve mollusc *Arctica islandica*. *Holocene*, 16, 967-974.

796 Scourse, J. D., Wanamaker, A. D., Weidman, C., Heinemeier, J., Reimer, P. J., Butler, P. G., Witbaard,
797 R. & Richardson, C. A. (2012). The marine radiocarbon bomb pulse across the temperate North
798 Atlantic: a compilation of delta C-14 time histories from *Arctica islandica* growth increments.
799 *Radiocarbon*, 54, 165-186.

800 Sejrup, H. P., Lehman, S. J., Hafliðason, H., Noone, D., Muscheler, R., Berstad, I. M. & Andrews, J. T.
801 (2010). Response of Norwegian Sea temperature to solar forcing since 1000 A.D. *Journal of*
802 *Geophysical Research*, 115.

803 Sicre, M.-A., Jacob, J., Ezat, U., Rousse, S., Kissel, C., Yiou, P., Eiriksson, J., Knudsen, K. L., Jansen,
804 E. & Turon, J.-L. (2008). Decadal variability of sea surface temperatures off North Iceland over
805 the last 2000 years. *Earth and Planetary Science Letters*, 268, 137-142.

806 Suess, H. E. (1953). *Natural radiocarbon and the rate of exchange of carbon dioxide between the*
807 *atmosphere and the sea. In: Aldrich, W. (Ed.), Nuclear Processes in Geologic Settings.*,
808 University of Chicago Press, Chicago,.

809 Swart, P. K., Greer, L., Rosenheim, B. E., Moses, C. S., Waite, A. J., Winter, A., Dodge, R. E. &
810 Helmle, K. (2010). The C-13 Suess effect in scleractinian corals mirror changes in the
811 anthropogenic CO₂ inventory of the surface oceans. *Geophysical Research Letters*, 37.

812 Swart, P.K., S. Torrold, A. Esienhauer, B. Rosenheim, C.G.A. Harrison, M. Grammer, and C. Latkoczy.
813 (2002). Intra-annual variation in the stable oxygen and carbon and trace element composition of
814 sclerosponges. *Paleoceanography* 17(3), 1029/2000PA000622.

815 Swart, P.K., R.E. Dodge, and J.H. Hudson. (1996). A 240-year stable oxygen and carbon isotopic record
816 in a coral from South Florida: Implications for the prediction of precipitation in southern Florida.
817 *Palaaios*, 11:362-375.

818 Tagliabue, A. & Bopp L. (2008). Towards understanding global variability in ocean carbon-13.
819 *Global Biogeochemical Cycles*, 22.

820 Trenberth, K. E. & Paolino, D. A. (1980). The northern hemisphere sea-level pressure data set - trends,
821 errors and discontinuities. *Monthly Weather Review*, 108, 855-872.

822 Trouet, V., Esper, J., Graham, N. E., Baker, A., Scourse, J. D. & Frank, D. C. (2009). Persistent positive
823 North Atlantic oscillation mode dominated the Medieval Climate Anomaly. *Science*, 324, 78-80.

824 Trouet, V. & Van Oldenborgh, G. J. (2013). climate explorer: a web-based research tool for high-
825 resolution paleoclimatology. *Tree-Ring Research*, 69, 3-13.

826 Ullman, D. J., McKinley, G. A., Bennington, V. & Dutkiewicz, S. (2009). Trends in the North Atlantic
827 carbon sink: 1992-2006. *Global Biogeochemical Cycles*, 23.

828 Vage, K., Pickart, R. S., Sarafanov, A., Knutsen, O., Mercier, H., Lherminier, P., Van Aken, H. M.,
829 Meincke, J., Quadfasel, D. & Bacon, S. (2011). The Irminger Gyre: Circulation, convection, and
830 interannual variability. *Deep-Sea Research Part I-Oceanographic Research Papers*, 58, 590-614.

831 Wanamaker, A. D., Jr., Butler, P. G., Scourse, J. D., Heinemeier, J., Eiriksson, J., Knudsen, K. L. &
832 Richardson, C. A. (2012). Surface changes in the North Atlantic meridional overturning
833 circulation during the last millennium. *Nat Commun*, 3, 899.

834 Wanamaker, A. D., Jr., Heinemeier, J., Scourse, J. D., Richardson, C. A., Butler, P. G., Eiriksson, J. &
835 Knudsen, K. L. (2008a). Very long-lived mollusks confirm 17th century ad tephra-based
836 radiocarbon reservoir ages for North Icelandic shelf waters. *Radiocarbon*, 50, 399-412.

837 Wanamaker, A. D., Kreutz, K. J., Schoene, B. R., Pettigrew, N., Borns, H. W., Introne, D. S., Belknap,
838 D., Maasch, K. A. & Feindel, S. (2008b). Coupled North Atlantic slope water forcing on Gulf of
839 Maine temperatures over the past millennium. *Climate Dynamics*, 31, 183-194.

840 Wanamaker, A. D., Kreutz, K. J., Schöne, B. R. & Introne, D. S. (2011). Gulf of Maine shells reveal
841 changes in seawater temperature seasonality during the Medieval Climate Anomaly and the Little
842 Ice Age. *Palaeogeography, Palaeoclimatology, Palaeoecology*, 302, 43-51.

Witbaard, R., Jenness, M. I., Vanderborg, K. & Ganssen, G. (1994). Verification of annual growth increments in *Arctica islandica* l from the north-sea by means of oxygen and carbon isotopes. *Netherlands Journal of Sea Research*, 33, 91-101.

Zeebe, R. E. & Wolf-Gladrow, D. (2001). *CO₂ in Seawater: Equilibrium, Kinetics, Isotopes, Volume 65 1st Edition*, Boston, Elsevier.

Figure and table legends

Figure 1: Schematic maps showing the main currents of A) the North Atlantic and B) the Icelandic region. The black star in B) denotes the shell sampling location. EGC = East Greenland Current; DWCZ = deep water convection zone; PF = Polar Front; SPG = Subpolar gyre; GS/NAC = Gulf Stream/North Atlantic Current; NIJ = North Icelandic Jet; NIIC = North Icelandic Irminger Current; EIC = East Icelandic Current; ICC = Icelandic circular current; SIC = South Iceland Current; IC = Irminger Current; ISC = Icelandic slope current. Figure adapted from Reynolds et al. (2016).

Figure 2: A) Standard error of the ontogenetically aligned $\delta^{13}\text{C}$ -shell data plotted against the corresponding sample depth (grey symbols represent individual ontogenetic ages and sample depth mean values respectively). The black line is an approximated best fit curve. The dashed grey line indicates the threshold of 0.1, below which the SE is relatively stable. B) Standardised population mean ontogenetic $\delta^{13}\text{C}$ curve plotted with associated standard error (shaded grey area). C) Mean population growth increment widths plotted by ontogenetic age. D) Sample depth given as the number of shells sampled in each ontogenetic year. The vertical dashed grey line denotes the position up to which the data are likely representative of the population mean ($N \geq 8$). E) Annually resolved $\delta^{13}\text{C}$ -shell anomalies fitted with a 10-year first order loess low pass filter (thin and thick black lines respectively). F) Plot of the slope (gradient, calculated as the first order differential) of the 10-year low pass filtered data (from panel E) calculated as the first order differential to indicate changes in the trend of the ontogenetically aligned $\delta^{13}\text{C}$ -shell data. Analysis of the slope identifies three distinct periods (indicated by the vertical dashed black lines).

Figure 3: A) Plot of the annually resolved $\delta^{13}\text{C}$ -shell record (grey line) spanning the period 953-2000 CE fitted with a 31-year running low pass filter (black line). B) Sample depth (number of shells sampled in a given year) of the annually resolved $\delta^{13}\text{C}$ -shell record. C) Mean and standard deviation (black line and grey bars respectively) of the $\delta^{13}\text{C}$ -shell data calculated over 50-year non-overlapping bins. The dashed blue and red lines represent the mean $\delta^{13}\text{C}$ -shell values calculated over the pre-industrial period (CE 953-1799) and over entire record respectively. D and E) Atmospheric and marine $\delta^{13}\text{C}$ curves derived from Law Dome ice cores, Antarctica (Francey et al., 1999) and tropical Atlantic corals and scleroponges (Bohm et al., 2002) respectively. F) Plot of the available annually resolved $\delta^{13}\text{C}$ -shell series from North Iceland (Flatey and Langanese 5 and 9; Schöne et al., 2011), the Gulf of Maine (Wanamaker et al., 2008) and North Atlantic $\delta^{13}\text{C}_{\text{DIC}}$ (Schöne et al., 2011). The annually resolved $\delta^{13}\text{C}$ records are shown with a polynomial line of best fit.

Table 1: Comparison between $\delta^{13}\text{C}$ trends contained in various marine proxy archives over the 20th century and the period from 1979-1999 during which there is, albeit patchy, observational $\delta^{13}\text{C}_{\text{DIC}}$ data available (Schöne et al., 2011). *The Isle of Man $\delta^{13}\text{C}$ series is decadal in resolution, despite being from *A. islandica*, as the samples were originally derived for radiocarbon analyses which requires larger sample sizes which ultimately constrains the minimum temporal resolution that can be obtained (Butler et al., 2009). **These series were not analysed over the instrumental period of 1979-1999 as they contained an insufficient number of samples over this period.

Figure 4: A) Multi-taper method spectral analysis and B) wavelet analysis of the $\delta^{13}\text{C}$ -shell record. The red line in panel A denotes the 95% significance level with respect to red noise. The masked area in panel B denotes the cone of influence, whilst the black lines highlight the 95% significance level.

Table 2: Table of the statistically significant ($P < 0.1$) spectral frequencies and periods identified in the $\delta^{13}\text{C}_{\text{shell}}$ record using multi taper method spectral analysis (Fig 7).

Figure 5: Spatial correlations calculated between the annually resolved $\delta^{13}\text{C}$ -shell record and A) mean April-June HadISST1 SSTs; B) mean December to February EN4 SSSs; C) mean July to September sea ice extent HadISST1 sea ice index D) mean December-February Trenberth sea level pressures (SLPs).

Figure 6: Comparison between A) the $\delta^{13}\text{C}$ -shell_{detrended} record (linear detrended); B) linear detrended HadISST1 SSTs; C) linear detrended EN4 SSSs; D) the wNAO index (plotted on an inverted y axis; Jones et al., 1997); and E) HadISST1 sea ice index plotted over the 20th century. F-I) lead-lag correlation analyses between the $\delta^{13}\text{C}$ -shell_{detrended} record and the HadISST1 SSTs, EN4 SSS, wNAO and HadISST1 sea ice index respectively. The dashed black lines in plots F-I correspond to the 95% significance level derived using the Ebisuzaki Monte Carlo methodology.

Figure 7: Comparison between contemporaneous proxy archives over the last millennium. A) the $\delta^{13}\text{C}$ -shell record; B) the North Icelandic $\delta^{18}\text{O}$ -shell record (Reynolds et al., 2016); C) the *A. islandica* RCS chronology (Butler et al., 2013); D) 100-year high pass filtered $\delta^{13}\text{C}$ -shell data; E) the north Icelandic ΔR series (Wanamaker et al., 2012); F) two wNAO indexes (Trouet et al., 2012; Ortega et al., 2015).

921
922
923

924

925

926
927
928
929
930
931

Table 1

Study	Archive	Location	20 th C trend	upper 95%	lower 95%	Analysis period
$\delta^{13}\text{C}$ -shell (this study)	<i>A. islandica</i>	Grimsey, Iceland	-0.003	-0.005	-0.001	1900-2000
Butler et al., 2009	<i>A. islandica</i>	Isle of Man	-0.003	-0.015	0.005	1903-1991
Schöne et al., 2011	<i>A. islandica</i>	Flatey, Iceland	-0.013	-0.015	-0.012	1900-1986
Schöne et al., 2011	<i>A. islandica</i>	Langanes 9, Iceland	-0.012	-0.013	-0.010	1945-2000
Schöne et al., 2011	<i>A. islandica</i>	Langanes 5, Iceland	-0.014	-0.015	-0.013	1900-2000
Wanamaker et al., 2008a/	<i>A. islandica</i>	Gulf of Maine	-0.007	-0.009	-0.006	1900-2000
Schöne et al., 2011						
Francey et al., 1999	Ice core	Greenland	-0.008	-0.010	-0.007	1905-1978
Böhn et al., 2002	Sclerosponge	Jamaica	-0.009	-0.010	-0.007	1906-1994
Böhn et al., 2002	Sclerosponge	Jamaica	-0.008	-0.009	-0.007	1902-1986
Böhn et al., 2002	Sclerosponge	Jamaica	-0.008	-0.009	-0.007	1901-1993
Böhn et al., 2002	Sclerosponge	Jamaica	-0.008	-0.010	-0.006	1904-1995
Böhn et al., 2002	Sclerosponge	Pedro Bank	-0.008	-0.009	-0.008	1905-1992
Swart et al., 2002	Coral	Bahamas	-0.011	-0.012	-0.010	1990-1992
Swart et al., 1996	Coral	Florida	-0.010	-0.013	-0.007	1900-1986
Cage and Austin, 2010	B. Foram.	Loch Sunart, Scotland	-0.006	-0.007	-0.005	1901-2000

			1979-1999 Trend	upper 95%	lower 95%	Analysis period
$\delta^{13}\text{C}_{\text{DIC}}$	observations	North Atlantic	-0.039	-0.048	-0.029	1979-1999
$\delta^{13}\text{C}$ -shell (this study)	<i>A. islandica</i>	Grimsey, Iceland	-0.039	-0.126	-0.026	1979-1999
Butler et al., 2009	<i>A. islandica</i>	Isle of Man		NAN**		
Schöne et al., 2011	<i>A. islandica</i>	Flatey, Iceland	0.064	0.029	0.157	1979-1986
Schöne et al., 2011	<i>A. islandica</i>	Langanes 9, Iceland	-0.016	-0.019	-0.012	1979-1999
Schöne et al., 2011	<i>A. islandica</i>	Langanes 5, Iceland	-0.027	-0.083	-0.018	1979-1999
Wanamaker et al., 2008a/	<i>A. islandica</i>	Gulf of Maine	-0.028	-0.033	-0.022	1979-1999
Schöne et al., 2011						
Francey et al., 1999	Ice core	Greenland		NAN**		
Bohn et al., 2002	Sclerosponge	Jamaica	-0.016	-0.019	-0.011	1981-1994
Böhn et al., 2002	Sclerosponge	Jamaica	-0.026	-0.033	-0.019	1979-1986
Böhn et al., 2002	Sclerosponge	Jamaica	-0.024	-0.028	-0.017	1980-1993
Böhn et al., 2002	Sclerosponge	Jamaica		NAN**		
Böhn et al., 2002	Sclerosponge	Pedro Bank	-0.020	-0.021	-0.017	1979-1992
Swart et al., 2002	Coral	Bahamas	-0.040	-0.130	-0.027	1979-1992
Swart et al., 1996	Coral	Florida	-0.148	-0.480	-0.080	1979-1986
Cage and Austin, 2010	B. Foram.	Loch Sunart, Scotland	-0.14	-0.046	-0.004	1980-1999

Table 2

Period	Frequency	Probability
524.00	0.0019	<0.01
120.47	0.0083	<0.05
8.39	0.1191	<0.1
5.42	0.1846	<0.05
4.56	0.2192	<0.1
2.04-4.31		<0.1

Figure 1

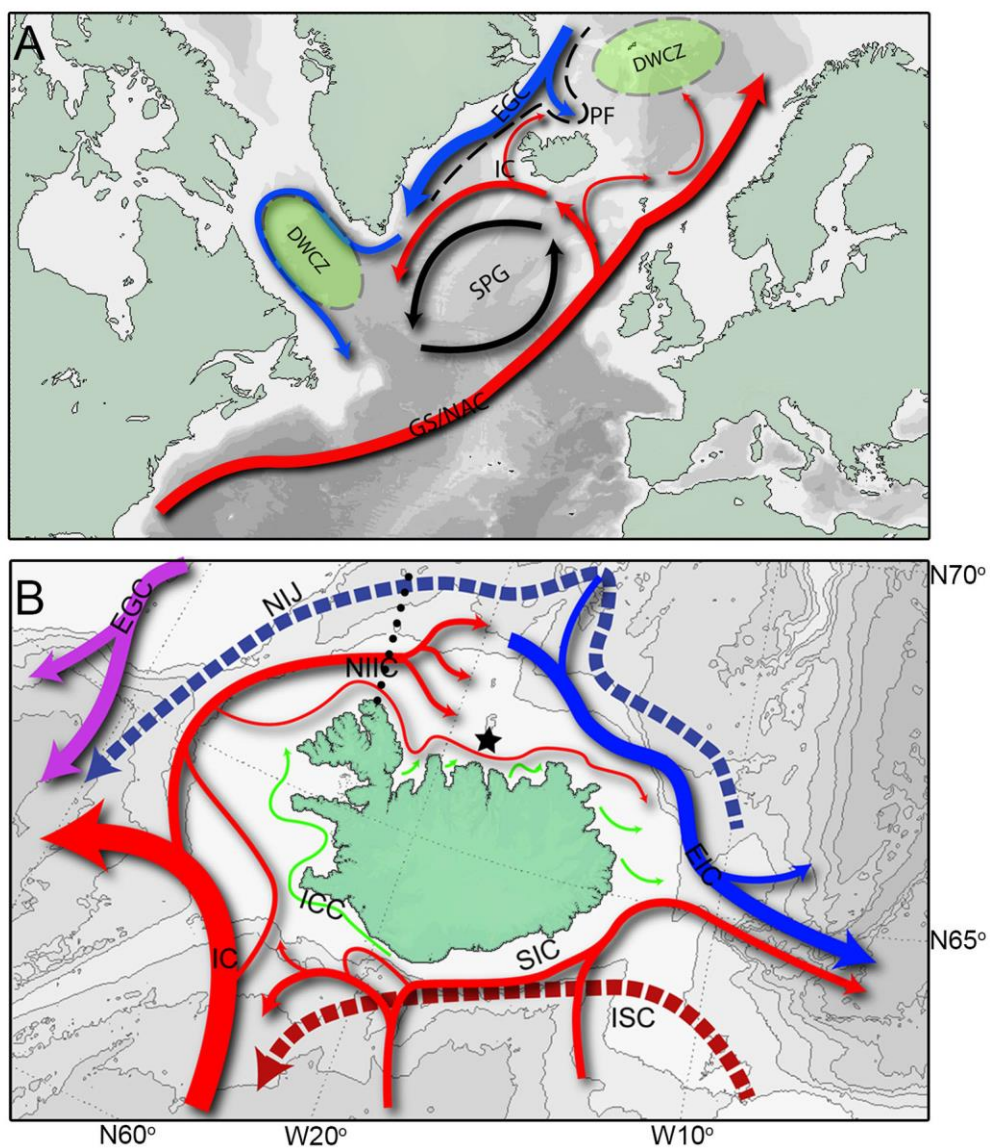
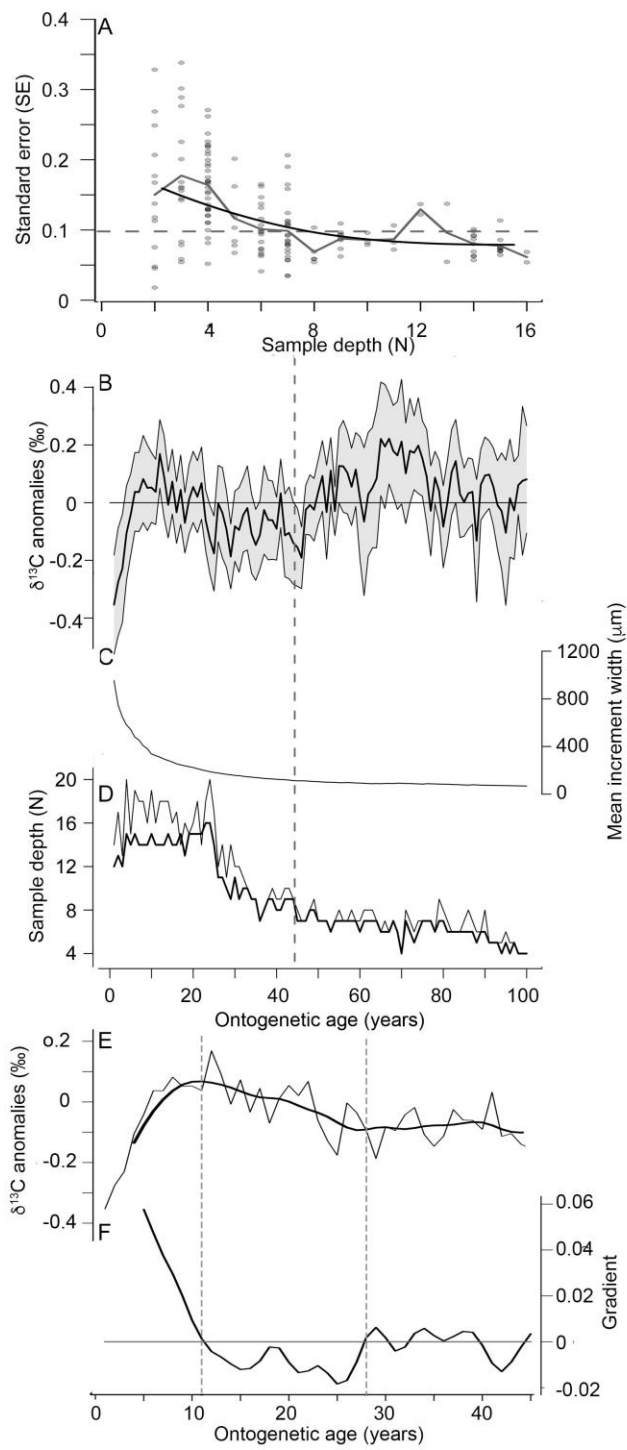
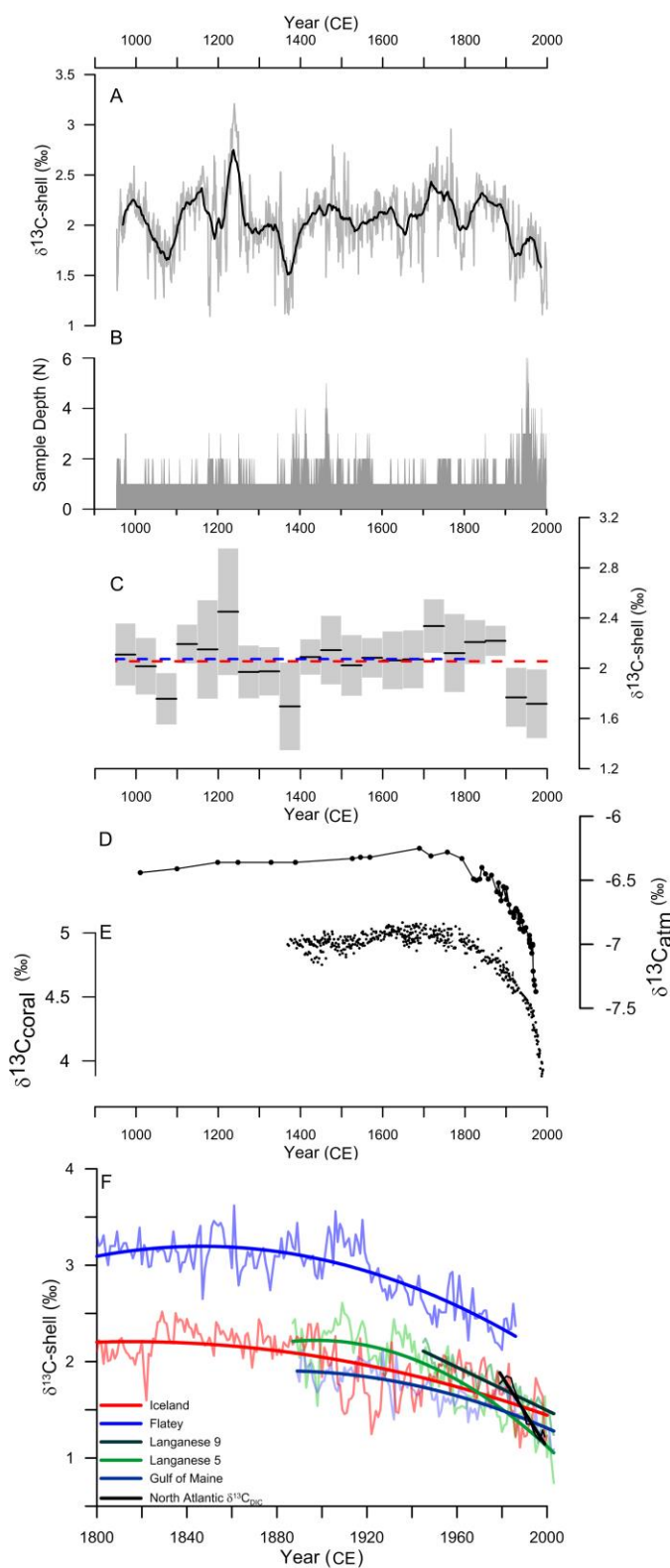


Figure 2



949 Figure 3



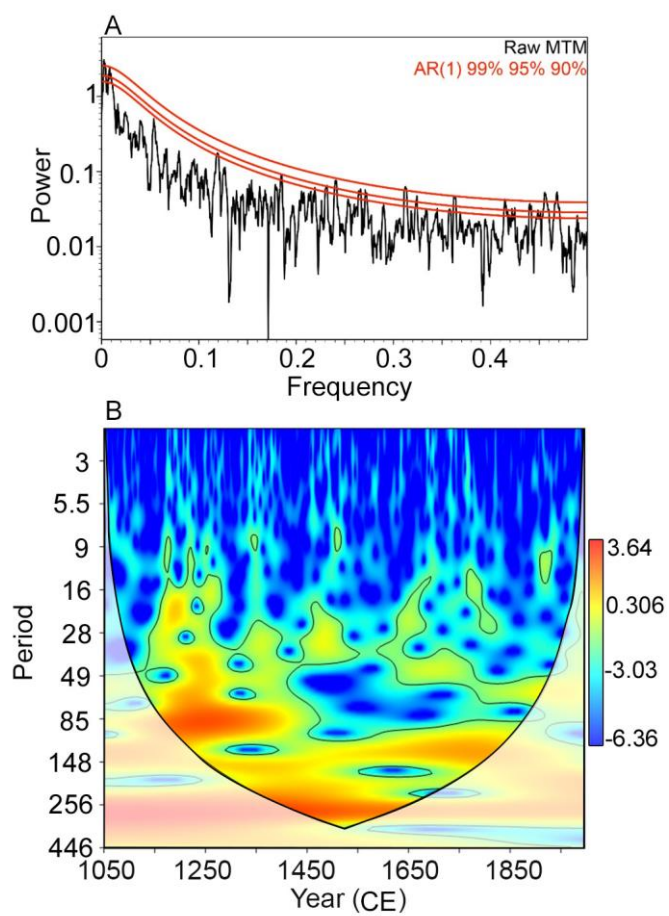
950

951

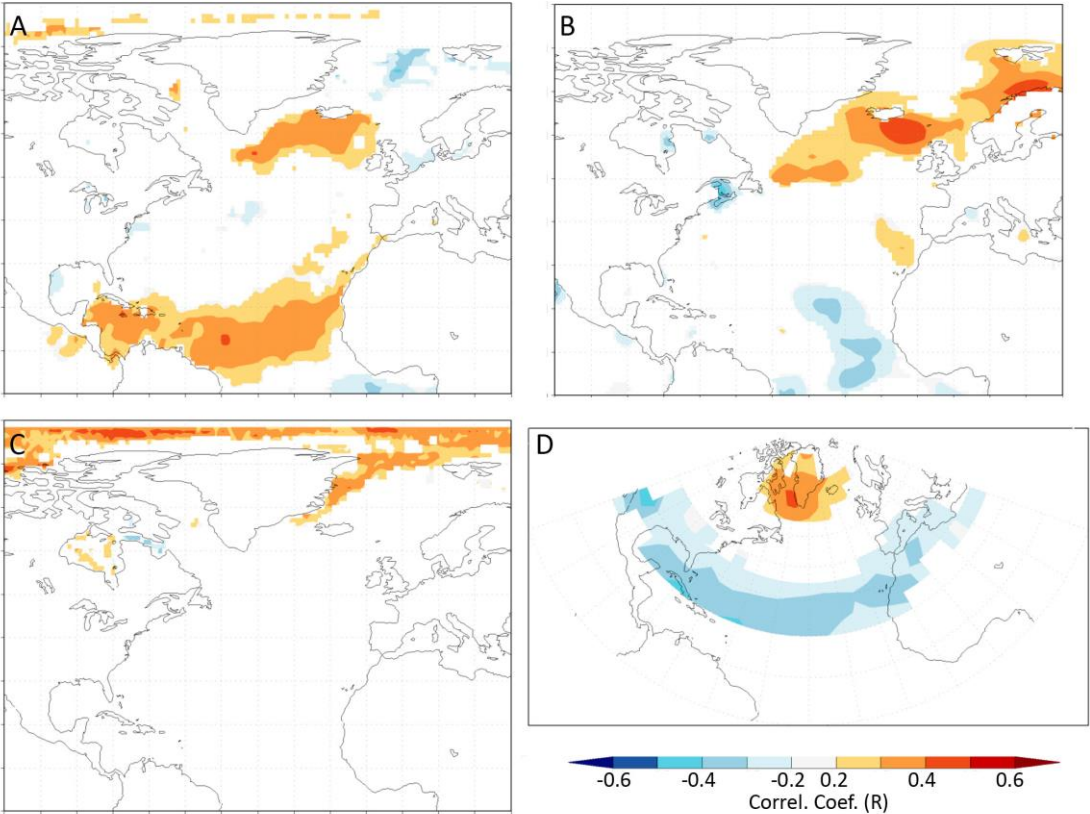
952

953

954 Figure 4

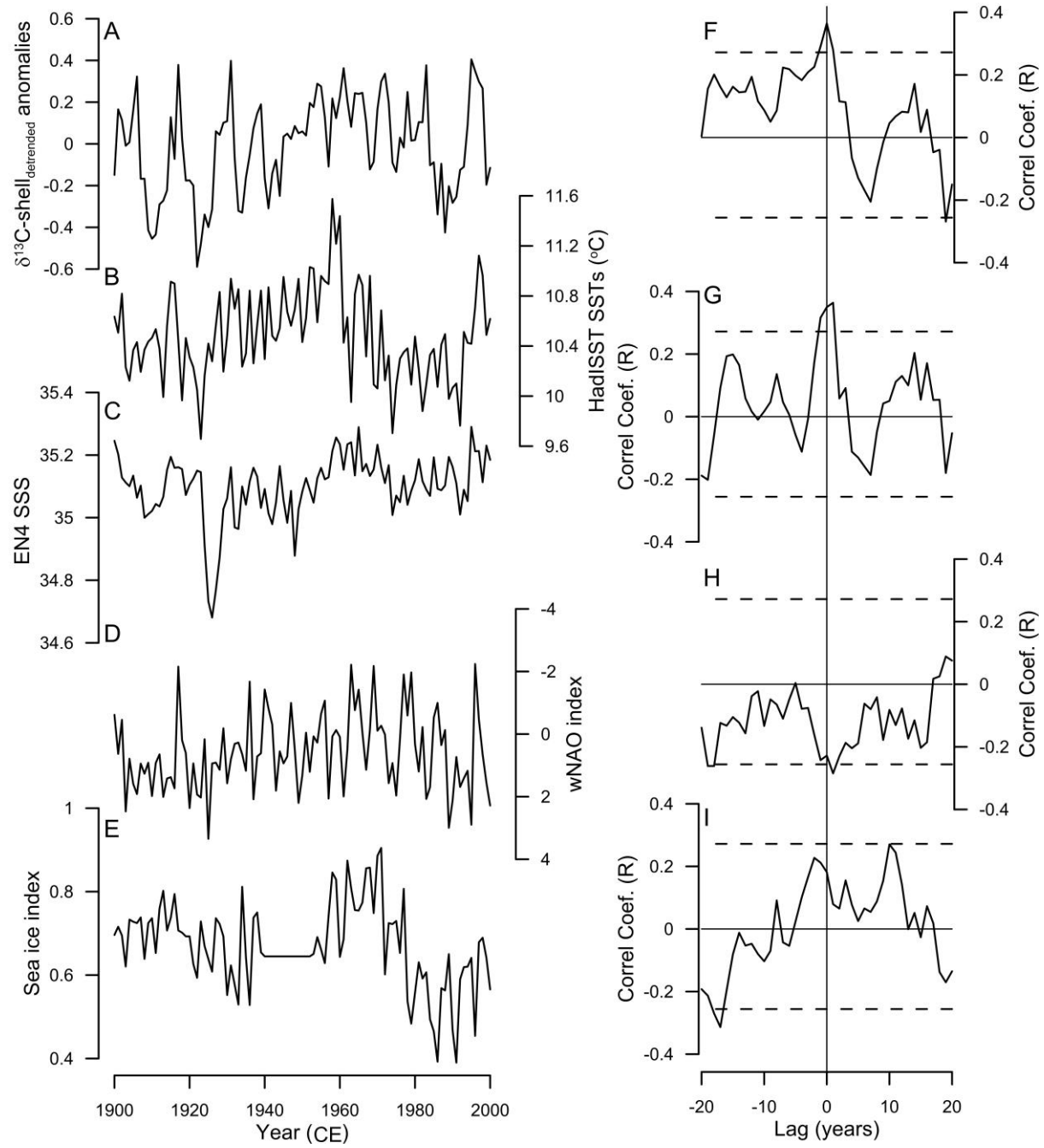


968 Figure 5



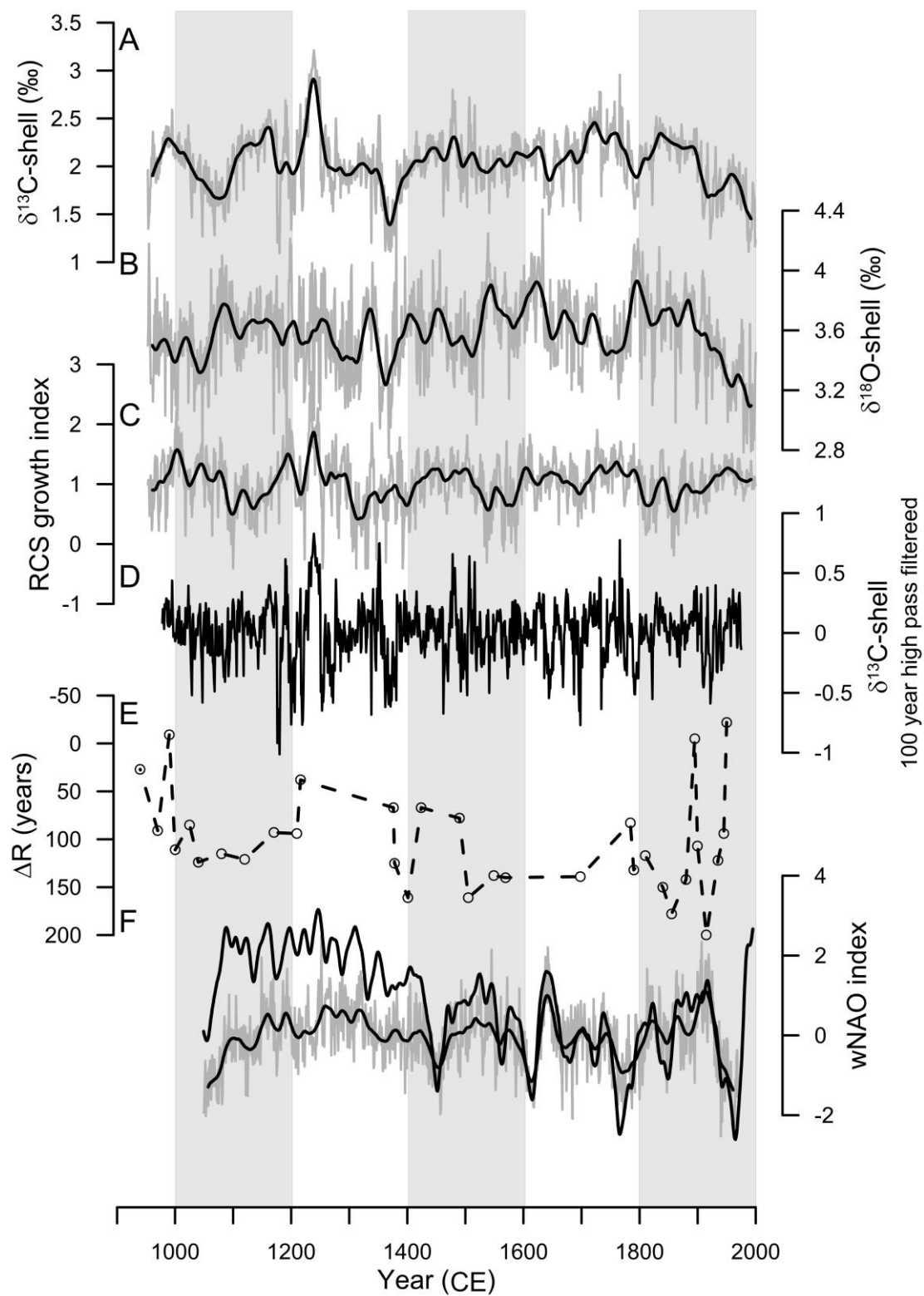
969
970
971
972
973
974
975
976
977
978
979
980
981

Figure 6



990 Figure 7

991



992